International Tables for Crystallography (2012). Vol. F, Chapter 2.1, pp. 45–63.

PART 2. BASIC CRYSTALLOGRAPHY

Chapter 2.1. Introduction to basic crystallography

J. Drenth

2.1.1. Crystals

It is always amazing to see how large molecules, such as proteins, nucleic acids and their complexes, order themselves so neatly in a crystalline arrangement. It is surprising because these large molecules have irregular surfaces with protrusions and cavities, and hydrophilic and hydrophobic spots. Nevertheless, they pack themselves into an orderly arrangement in crystals of millimetre sizes.

Crystals of biological macromolecules are, like most other crystals, not ideal. The X-ray diffraction pattern fades away at diffraction angles corresponding to lattice-plane distances between 1 and 2 Å or even worse. This is not so surprising, since protein crystals are relatively soft. The interaction energy between protein molecules in crystals is of the order of 63×10^{-21} J per protein molecule, or approximately 15 kT (Haas & Drenth, 1995). This corresponds to about ten hydrogen bonds, four salt bridges, or a 400 Å^2 buried hydrophobic surface. Although this energy might not be very different from crystalline interactions between small molecules, the large size of the protein molecules or macromolecular assemblies makes the crystals much more sensitive to distorting forces. Irregularities in the crystal lattice can also stem from the incorporation of impurities – either foreign substances or slightly denatured molecules from the parent protein. Moreover, some molecules may be incorrectly oriented, because the difference in interaction energy between different orientations is rather small. Also, amino-acid side chains assume more than one conformation. These are static irregularities. In addition, dynamic disorder exists: parts of the macromolecule are flexible and affect the X-ray diffraction pattern just as the temperature does.

By neglecting distortions caused by lattice imperfections, crystals are found to have a repeating unit, the unit cell, with basis vectors **a**, **b** and **c**, and angles α, β and γ between them (Fig. 2.1.1.1). The enormous number of unit cells in a crystal are stacked in three dimensions, in an orderly way, with the origins of the unit cells forming a grid or lattice. In Fig. 2.1.1.2, part of a crystalline lattice containing $5 \times 3 \times 3$ unit cells is drawn.

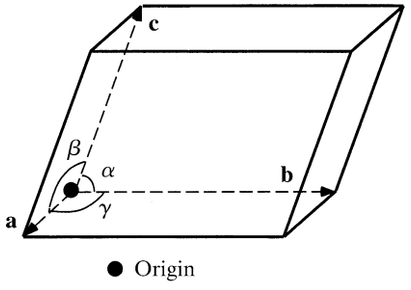

Figure 2.1.1.1
One unit cell with axes **a**, **b** and **c**. The angles between the axes are α, β and γ. Note that the axial system is right-handed. Reproduced with permission from Drenth (1999). Copyright (1999) Springer-Verlag.

It is customary to call the direction along the unit-cell vector **a** the x direction in the lattice; similarly, y is along **b**, and z along **c**.

Crystallographers use a simple system to indicate the planes in a crystal lattice. For instance, the plane containing the unit-cell vectors **a** and **b** is called (001), and the plane containing the vectors **b** and **c** is called (100). The plane (010) contains the vectors **a** and **c**. It should be pointed out that these planes are not limited to one unit cell, but extend through the entire crystal. Moreover, each of these three planes is only one member of a set of parallel and equidistant planes: the set (001), the set (100) and the set (010). For each set, the lattice planes pass through all lattice points, where the lattice points are at the corners of the unit cells (see Fig. 2.1.1.2). Besides the sets of planes (001), (100) and (010), many more sets of parallel and equidistant planes can be drawn through the lattice points. In Fig. 2.1.1.3, this is done for a two-dimensional lattice. Lattice planes always divide the unit-cell vectors **a**, **b** and **c** into a number of equal parts. If the lattice planes divide the **a** vector of the unit cell into h equal parts, the first index for this set of planes is h. The second index, k, is related to the division of **b**, and the third index, l, to the division of **c**. If the set of lattice planes is parallel to a basis unit-cell vector, the corresponding index is 0. Indices for lattice planes are given in parentheses. They should not be confused with directions of vectors connecting lattice points; these are given in square brackets: [uvw], where u is the coordinate in the **a** direction expressed as the number of **a**'s, v in the **b** direction expressed as the number of **b**'s and w in the **c** direction expressed as the number of **c**'s. u, v and w are taken as the simplest set of whole numbers. For instance, [100] is along **a**; [200] has the same direction, but [100] is used instead. [111] points from the origin to the opposite corner of the unit cell.

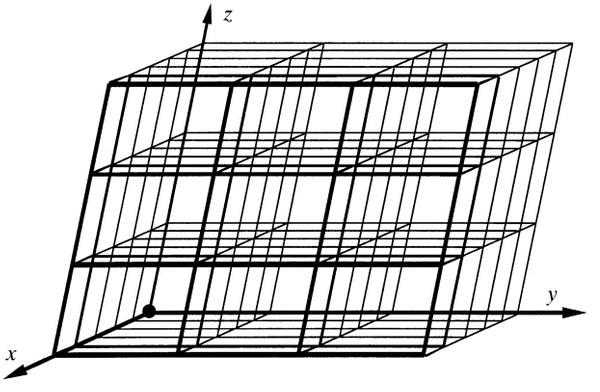

Figure 2.1.1.2
A set of $5 \times 3 \times 3$ unit cells. The points where the lines intersect are called lattice points. The axes x and y form a (001) plane, which is one member of the set of parallel and equidistant (001) planes; y and z form a (100) plane, and z and x a (010) plane. Reproduced with permission from Drenth (1999). Copyright (1999) Springer-Verlag.

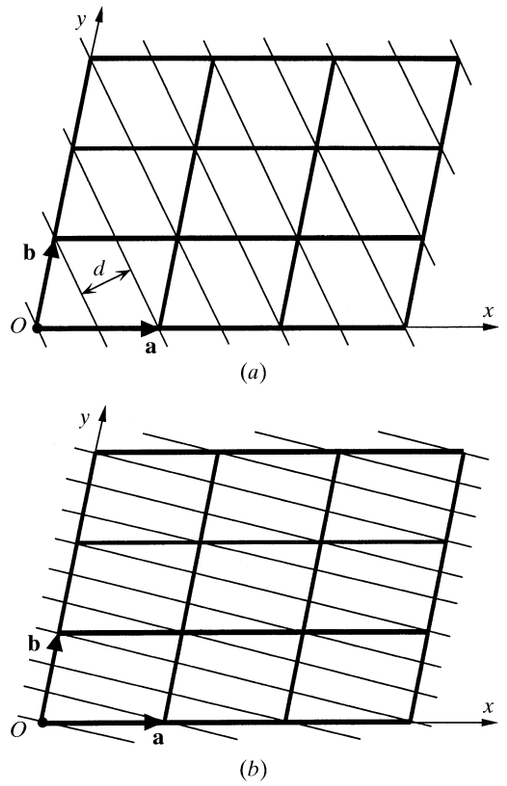

Figure 2.1.1.3
A two-dimensional lattice with 3 × 3 unit cells. In both (*a*) and (*b*), a set of equidistant parallel lattice planes is drawn. They pass through all lattice points. Lattice planes always divide the unit-cell axes into a whole number of equal parts – 1, 2, 3 *etc*. For instance, in (*a*), the vector **a** of the unit cell is cut into two parts, and the vector **b** into only one part. This set of planes is then given the indices $h = 2$ and $k = 1$. In three dimensions, there would be a third index, *l*. In (*b*), the set of lattice planes has the indices $h = 1$ and $k = 3$. In general, lattice planes have the indices (*hkl*), known as Miller indices. If a set of lattice planes is parallel to an axis, the corresponding index is 0. For instance, (001) is the set of planes parallel to the unit-cell vectors **a** and **b**. Note that the projection of $\mathbf{a}/h$ on the line normal to the lattice plane is equal to the lattice-plane distance *d*. This is also true for $\mathbf{b}/k$. Reproduced with permission from Drenth (1999). Copyright (1999) Springer-Verlag.

The choice of the unit cell is not unique and, therefore, guidelines have been established for selecting the standard basis vectors and the origin. They are based on symmetry and metric considerations:

(1) The axial system should be right-handed.
(2) The basis vectors should coincide as much as possible with directions of highest symmetry.
(3) The cell taken should be the smallest one that satisfies condition (2).
(4) Of all lattice vectors, none is shorter than **a**.
(5) Of those not directed along **a**, none is shorter than **b**.
(6) Of those not lying in the *ab* plane, none is shorter than **c**.
(7) The three angles between the basis vectors **a**, **b** and **c** are either all acute (<90°) or all obtuse (≥90°).

It should be noted that the rules for choosing **a**, **b** and **c** are not always obeyed, because of other conventions (see Section 2.1.3). Condition (3) sometimes leads to a centred unit cell instead of a primitive cell. Primitive cells have only one lattice point per unit cell, whereas non-primitive cells contain two or more lattice points. They are designated *A*, *B* or *C* if opposite faces of the cell are centred: *A* for *bc* centring, *B* for *ac* centring and *C* for *ab* centring. If all faces are centred, the designation is *F*, and if the cell is body-centred, it is *I* (Fig. 2.1.1.4).

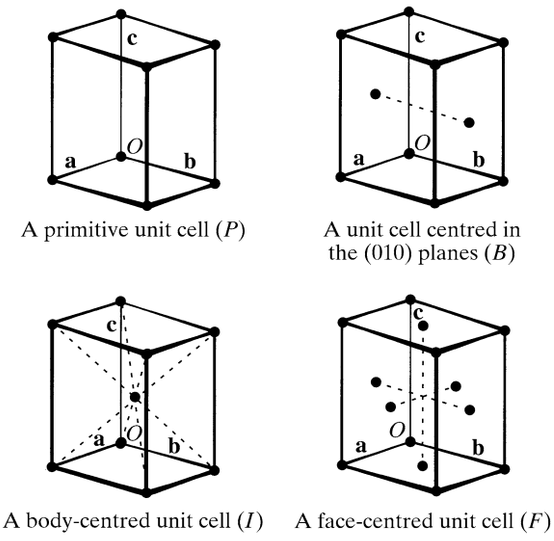

Figure 2.1.1.4
Non-centred and centred unit cells. Reproduced with permission from Drenth (1999). Copyright (1999) Springer-Verlag.

2.1.2. Symmetry

A symmetry operation can be defined as an operation which, when applied, results in a structure indistinguishable from the original one. According to this definition, the periodic repetition along **a**, **b** and **c** represents translational symmetry.

In addition, rotational symmetry exists, but only rotational angles of 60, 90, 120, 180 and 360° are allowed (*i.e*. rotation over 360/*n* degrees, where *n* is an integer). These correspond to *n*-fold rotation axes, with $n = 6, 4, 3, 2$ and 1 (identity), respectively. Rotation axes with $n = 5$ or $n > 6$ are not found as crystallographic symmetry axes, because translations of unit cells containing these axes do not completely fill three-dimensional space. Another type of rotational symmetry axis is the screw axis. It combines a rotation with a translation. For a twofold screw axis, the translation is over 1/2 of the unit-cell length in the direction of the axis; for a threefold screw axis, it is 1/3 or 2/3 *etc*. In this way, the translational symmetry operators can be obeyed. The requirement that translations are 1/2, 1/3, 2/3 *etc*. of the unit-cell length does not exist for individual objects that are not related by crystallographic translational symmetry operators. For instance, an α-helix has 3.6 residues per turn.

Besides translational and rotational symmetry operators, mirror symmetry and inversion symmetry exist. Mathematically, it can be proven that not all combinations of symmetry elements are allowed, but that 230 different combinations can occur. They are the space groups which are discussed extensively in *IT* A (2005). The graphical and printed symbols for the symmetry elements are also found in *IT* A (Chapter 1.4).

Biological macromolecules consist of building blocks such as amino acids or sugars. In general, these building-block structures are not symmetrical and the mirror images of the macromolecules do not exist in nature. Space groups with mirror planes and/or inversion centres are not allowed for crystals of these molecules, because these symmetry operations interchange right and left hands. Biological macromolecules crystallize in one of the 65 enantiomorphic space groups. (Enantiomorphic means the structure is not superimposable on its mirror image.) Apparently, some of these space groups supply more favourable packing conditions for proteins than others. The most favoured space group is $P2_12_12_1$ (Table 2.1.2.1). A consequence of symmetry is

Table 2.1.2.1
The most common space groups for protein crystals

Situation as of April 1997; data extracted from the Protein Data Bank and supplied by Rob Hooft, EMBL Heidelberg.

Space group	Occurrence (%)
$P2_12_12_1$	23
$P2_1$	11
$P3_221$	8
$P2_12_12$	6
$C2$	6

that multiple copies of particles exist in the unit cell. For instance, in space group $P2_1$ (space group No. 4), one can always expect two exactly identical entities in the unit cell, and one half of the unit cell uniquely represents the structure. This unique part of the structure is called the asymmetric unit. Of course, the asymmetric unit does not necessarily contain one protein molecule. Sometimes the unit cell contains fewer molecules than anticipated from the number of asymmetric units. This happens when the molecules occupy a position on a crystallographic axis. This is called a special position. In this situation, the molecule itself obeys the axial symmetry. Otherwise, the molecules in an asymmetric unit are on general positions. There may also be two, three or more equal or nearly equal molecules in the asymmetric unit related by noncrystallographic symmetry.

2.1.3. Point groups and crystal systems

If symmetry can be recognized in the external shape of a body, like a crystal or a virus molecule, corresponding symmetry elements have no translations, because internal translations (if they exist) do not show up in macroscopic properties. Moreover, they pass through one point, and this point is not affected by the symmetry operations (point-group symmetry). For idealized crystal shapes, the symmetry axes are limited to one-, two-, three-, four- and sixfold rotation axes because of the space-filling

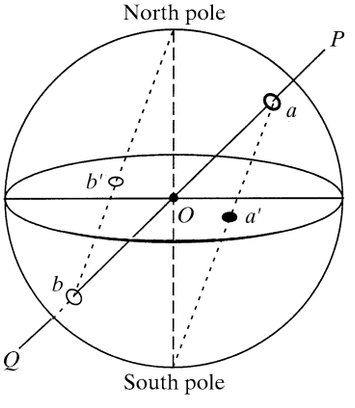

Figure 2.1.3.1
How to construct a stereographic projection. Imagine a sphere around the crystal with O as the centre. O is also the origin of the coordinate system of the crystal. Symmetry elements of the point groups pass through O. Line OP is normal to a crystal plane. It cuts through the sphere at point a. This point a is projected onto the horizontal plane through O in the following way: a vertical dashed line is drawn through O normal to the projection plane and connecting a north and a south pole. Point a is connected to the pole on the other side of the projection plane, the south pole, and is projected onto the horizontal plane at a'. For a normal OQ intersecting the lower part of the sphere, the point of intersection b is connected to the north pole and projected at b'. For the symmetry elements, their points of intersection with the sphere are projected onto the horizontal plane.

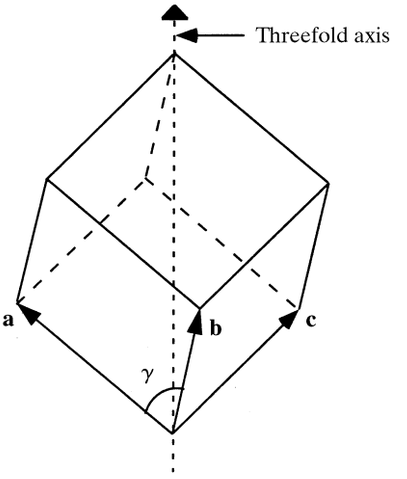

Figure 2.1.3.2
A rhombohedral unit cell.

requirement for crystals. With the addition of mirror planes and inversion centres, there are a total of 32 possible crystallographic point groups.

Not all combinations of axes are allowed. For instance, a combination of two twofold axes at an arbitrary angle with respect to each other would multiply to an infinite number of twofold axes. A twofold axis can only be combined with another twofold axis at 90°. A third twofold axis is then automatically produced perpendicular to the first two (point group 222). In the same way, a threefold axis can only be combined with three twofold axes perpendicular to the threefold axis (point group 32).

For crystals of biological macromolecules, point groups with mirrors or inversion centres are not allowed, because these molecules are chiral. This restricts the number of crystallographic point groups for biological macromolecules to 11; these are the enantiomorphic point groups and are presented in Table 2.1.3.1.

Although the crystals of asymmetric molecules can only belong to one of the 11 enantiomorphic point groups, it is nevertheless important to be aware of the other point groups, especially the 11 centrosymmetric ones (Table 2.1.3.2). This is because if anomalous scattering can be neglected, the X-ray diffraction pattern of a crystal is always centrosymmetric, even if the crystal itself is asymmetric (see Sections 2.1.7 and 2.1.8).

The protein capsids of spherical virus molecules have their subunits packed in a sphere with icosahedral symmetry (532). This is the symmetry of a noncrystallographic point group (Table 2.1.3.3). A fivefold axis is allowed because translation symmetry does not apply to a virus molecule. Application of the 532 symmetry leads to 60 identical subunits in the sphere. This is the simplest type of spherical virus (triangulation number $T = 1$). Larger numbers of subunits can also be incorporated in this icosahedral surface lattice, but then the subunits lie in quasi-equivalent environments and T assumes values of 3, 4 or 7. For instance, for $T = 3$ particles there are 180 identical subunits in quasi-identical environments.

On the basis of their symmetry, the point groups are subdivided into crystal systems as follows. For each of the point groups, a set of axes can be chosen displaying the external symmetry of the crystal as clearly as possible, and, in this way, the seven crystal systems of Table 2.1.3.4 are obtained. If no other symmetry is present apart from translational symmetry, the crystal belongs to the triclinic system. With one twofold axis or screw axis, it is monoclinic. The convention in the monoclinic system is to choose the b axis along the twofold axis. The orthorhombic system

Table 2.1.3.1
The 11 enantiomorphic point groups

The point groups are presented as two stereographic projections (see Fig. 2.1.3.1). On the right is a projection of the symmetry elements, and on the left a projection of the general faces. They are arranged according to the crystal system to which they belong: triclinic, monoclinic *etc*. Different point groups are separated by full horizontal rules. The monoclinic point groups are given in two settings: in the conventional setting with the twofold axis along **b** (unique axis *b*), and the other setting with unique axis *c*. The *b* axis is horizontal in the projection plane, and the *c* axis is normal to the plane. Three-, four- and sixfold axes are always set along the *c* axis, normal to the plane. A special case is the trigonal system; either hexagonal axes or rhombohedral axes can be chosen. In the hexagonal case, the threefold axis is along the *c* axis. The other two axes are chosen along or between the twofold axes, which include an angle of 120°. In the rhombohedral setting, the threefold axis is along the body diagonal of the unit cell, and the unit cell vectors **a**, **b** and **c** are the shortest non-coplanar lattice vectors symmetrically equivalent with respect to the threefold axis (Fig. 2.1.3.2). Symbols:

- General face above the plane
- General face below the plane
- Twofold rotation axis
- Threefold rotation axis
- Fourfold rotation axis
- Sixfold rotation axis

Adapted with permission from *IT* A (2005), Table 10.1.2.2.

TRICLINIC	1	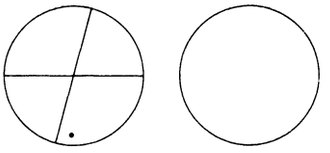
MONOCLINIC	2	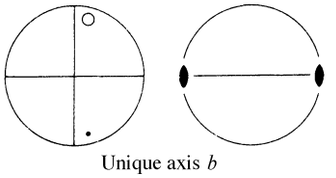 Unique axis *b* 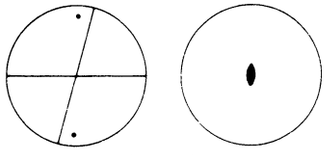 Unique axis *c*
ORTHORHOMBIC	222	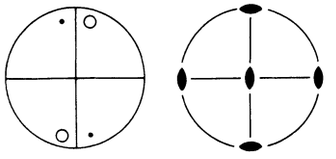
TETRAGONAL	4	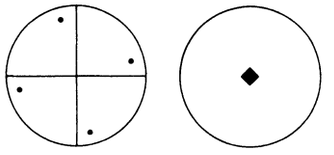
TETRAGONAL	422	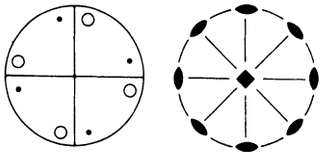

Table 2.1.3.1 (continued)

TRIGONAL Hexagonal axes	3	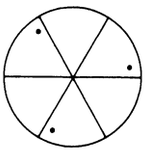	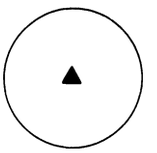
TRIGONAL Rhombohedral axes	3	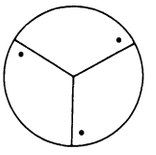	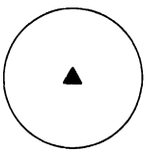
TRIGONAL Hexagonal axes	321	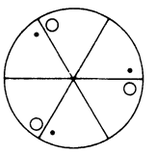	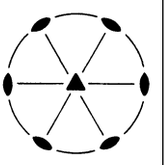
TRIGONAL Hexagonal axes	312	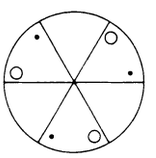	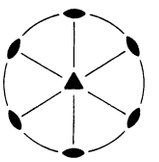
TRIGONAL Rhombohedral axes	32	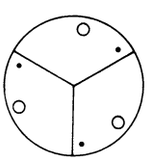	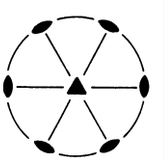
HEXAGONAL	6	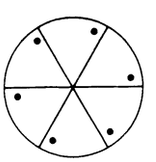	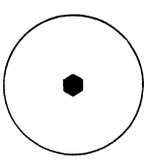
HEXAGONAL	622	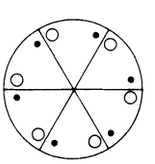	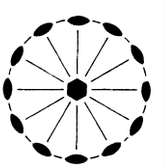
CUBIC	23	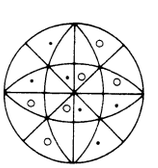	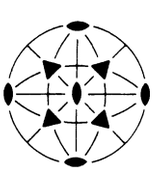
CUBIC	432	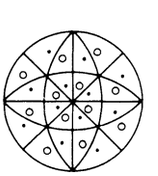	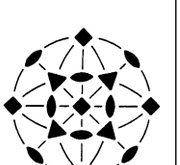

Table 2.1.3.2
The 11 point groups with a centre of symmetry

For details see Table 2.1.3.1. Projections of mirror planes are indicated by a bold line or circle. The inversion centre ($\bar{1}$) is indicated by a small circle at the origin. Adapted with permission from *IT* A (2005), Table 10.1.2.2.

TRICLINIC	$\bar{1}$	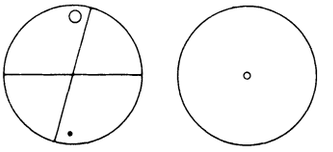
MONOCLINIC	2/*m*	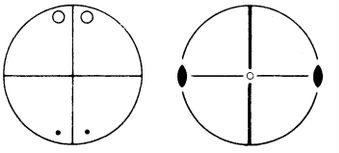 Unique axis *b* 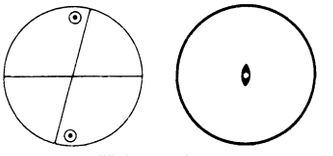 Unique axis *c*
ORTHORHOMBIC	*mmm* or $\frac{2}{m}\frac{2}{m}\frac{2}{m}$	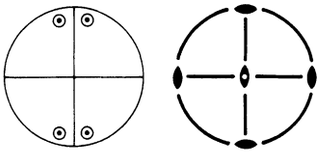
TETRAGONAL	4/*m*	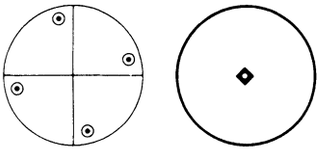
TETRAGONAL	4/*mmm* or $\frac{4}{m}\frac{2}{m}\frac{2}{m}$	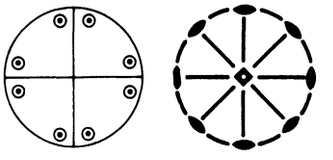
TRIGONAL Hexagonal axes	$\bar{3}$	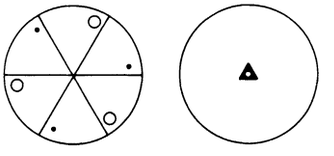
TRIGONAL Rhombohedral axes	$\bar{3}$	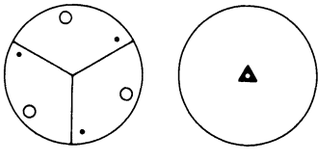

Table 2.1.3.2 (continued)

TRIGONAL Hexagonal axes	$\bar{3}m1$ or $\bar{3}\frac{2}{m}1$	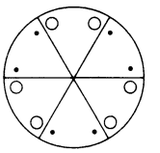	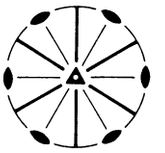
TRIGONAL Hexagonal axes	$\bar{3}1m$ or $\bar{3}1\frac{2}{m}$	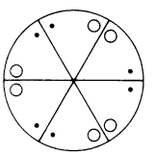	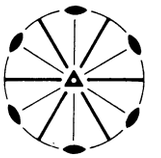
TRIGONAL Rhombohedral axes	$\bar{3}m$ or $\bar{3}\frac{2}{m}$	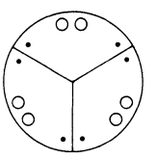	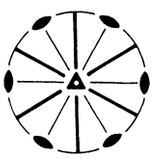
HEXAGONAL	$6/m$	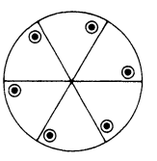	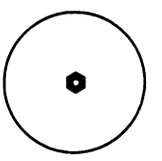
HEXAGONAL	$6/mmm$ or $\frac{6}{m}\frac{2}{m}\frac{2}{m}$	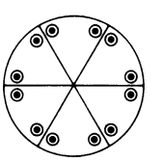	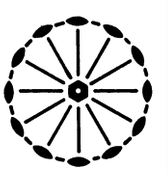
CUBIC	$m\bar{3}$ or $\frac{2}{m}\bar{3}$	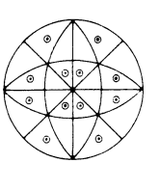	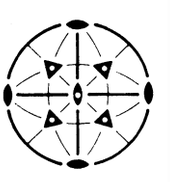
CUBIC	$m\bar{3}m$ or $\frac{4}{m}\bar{3}\frac{2}{m}$	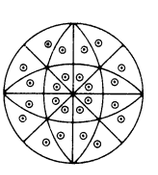	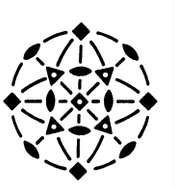

Table 2.1.3.3
The icosahedral point group 532

For details see Table 2.1.3.1. Adapted with permission from *IT* A (2005), Table 10.1.4.3.

ICOSAHEDRAL	532	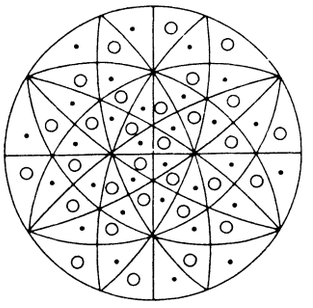	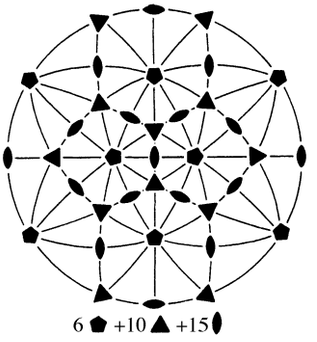

Table 2.1.3.4
The seven crystal systems

Crystal system	Conditions imposed on cell geometry	Minimum point-group symmetry
Triclinic	None	1
Monoclinic	Unique axis b: $\alpha = \gamma = 90^\circ$	2
Orthorhombic	$\alpha = \beta = \gamma = 90^\circ$	222
Tetragonal	$a = b$; $\alpha = \beta = \gamma = 90^\circ$	4
Trigonal	Hexagonal axes: $a = b$; $\alpha = \beta = 90^\circ$; $\gamma = 120^\circ$	3
	Rhombohedral axes: $a = b = c$; $\alpha = \beta = \gamma$ †	
Hexagonal	$a = b$; $\alpha = \beta = 90^\circ$; $\gamma = 120^\circ$	6
Cubic	$a = b = c$; $\alpha = \beta = \gamma = 90^\circ$	23

† A rhombohedral unit cell can be regarded as a cube extended or compressed along the body diagonal (the threefold axis) (see Fig. 2.1.3.2).

has three mutually perpendicular twofold (screw) axes. Another convention is that in tetragonal, trigonal and hexagonal crystals, the axis of highest symmetry is labelled c. These conventions can deviate from the guide rules for unit-cell choice given in Section 2.1.1.

The seven crystal systems are based on the point-group symmetry. Except for the triclinic unit cell, all other cells can occur either as primitive unit cells or as centred unit cells (Section 2.1.1). A total of 14 different types of unit cell exist, depicted in Fig. 2.1.3.3. Their corresponding crystal lattices are commonly called Bravais lattices.

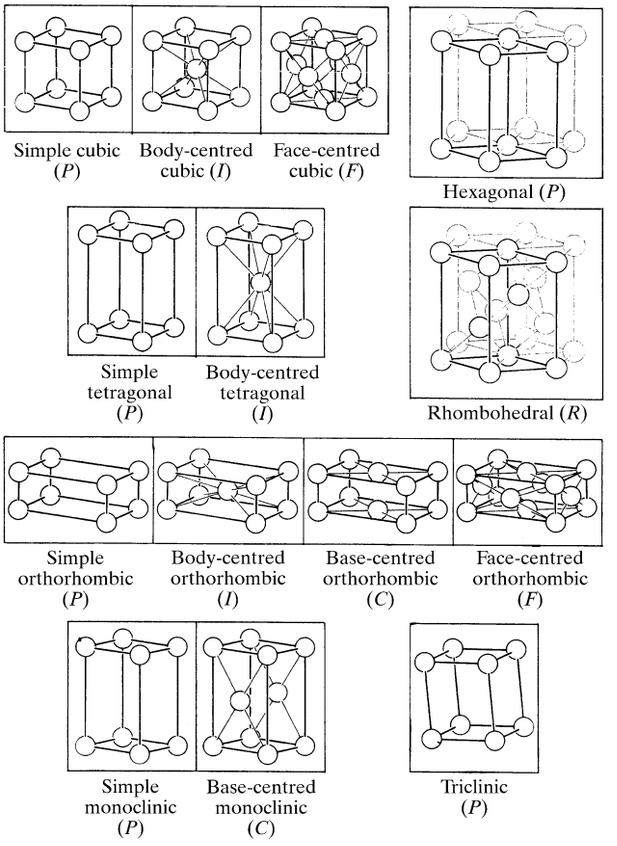

Figure 2.1.3.3
The 14 Bravais lattices. Reproduced with permission from Burzlaff & Zimmermann (2005).

2.1.4. Basic diffraction physics

2.1.4.1. Diffraction by one electron

The scattering of an X-ray beam by a crystal results from interaction between the electric component of the beam and the electrons in the crystal. The magnetic component has hardly any effect and can be disregarded.

If a monochromatic polarized beam hits an electron, the electron starts to oscillate in the direction of the electric vector of the incident beam (Fig. 2.1.4.1). This oscillating electron acts as the aerial of a transmitter and radiates X-rays with the same or lower frequency as the incident beam. The frequency change is due to the Compton effect: the photons of the incident beam collide with the electron and lose part of their energy. This is inelastic scattering, and the scattered radiation is incoherent with the incident beam. Compton scattering contributes to the background in a diffraction experiment. In elastic scattering, the scattered radiation has the same wavelength as the incident

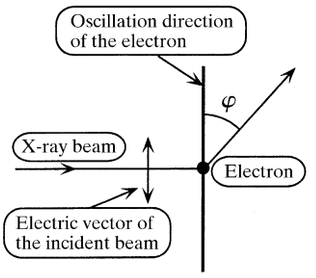

Figure 2.1.4.1
The electric vector of a monochromatic and polarized X-ray beam is in the plane. It hits an electron, which starts to oscillate in the same direction as the electric vector of the beam. The oscillating electron acts as a source of X-rays. The scattered intensity depends on the angle φ between the oscillation direction of the electron and the scattering direction [equation (2.1.4.1)]. Reproduced with permission from Drenth (1999). Copyright (1999) Springer-Verlag.

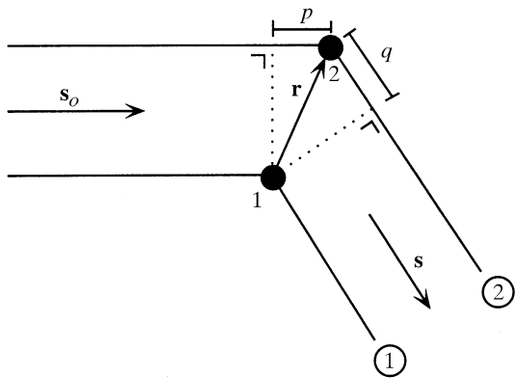

Figure 2.1.4.2
The black dots are electrons. The origin of the system is at electron 1; electron 2 is at position **r**. The electrons are irradiated by an X-ray beam from the direction indicated by vector $\mathbf{s}_o$. The radiation scattered by the electrons is observed in the direction of vector **s**. Because of the path difference $p + q$, scattered beam 2 will lag behind scattered beam 1 in phase. Reproduced with permission from Drenth (1999). Copyright (1999) Springer-Verlag.

radiation, and this is the radiation responsible for the interference effects in diffraction. It was shown by Thomson that if the electron is completely free the following hold:

(1) The phase difference between the incident and the scattered beam is π, because the scattered radiation is proportional to the displacement of the electron, which differs by π in phase with its acceleration imposed by the electric vector.
(2) The amplitude of the electric component of the scattered wave at a distance r which is large in comparison with the wavelength of the radiation is

$$E_{\rm el} = E_o \frac{1}{r} \frac{e^2}{mc^2} \sin\varphi,$$

where E_o is the amplitude of the electric vector of the incident beam, e is the electron charge, m is its mass, c is the speed of light and φ is the angle between the oscillation direction of the electron and the scattering direction (Fig. 2.1.4.1). Note that $E_o \sin\varphi$ is the component of E_o perpendicular to the scattering direction.

In terms of energy,

$$I_{\rm el} = I_o \frac{1}{r^2} \left(\frac{e^2}{mc^2}\right)^2 \sin^2\varphi. \qquad (2.1.4.1a)$$

The scattered energy per unit solid angle is

$$I_{\rm el}(\Omega = 1) = I_{\rm el} r^2. \qquad (2.1.4.1b)$$

It was shown by Klein & Nishina (1929) [see also Heitler (1966)] that the scattering by an electron can be discussed in terms of the classical Thomson scattering if the quantum energy $h\nu \ll mc^2$. This is not true for very short X-ray wavelengths. For $\lambda = 0.0243$ Å, $h\nu$ and mc^2 are exactly equal, but for $\lambda = 1.0$ Å, $h\nu$ is 0.0243 times mc^2. Since wavelengths in macromolecular crystallography are usually in the range 0.8–2.5 Å, the classical approximation is allowed. It should be noted that:

(1) The intensity scattered by a free electron is independent of the wavelength.
(2) Thomson's equation can also be applied to other charged particles, *e.g.* a proton. Because the mass of a proton is 1800 times the electron mass, scattering by protons and by atomic nuclei can be neglected.
(3) Equation (2.1.4.1*a*) gives the scattering for a polarized beam. For an unpolarized beam, $\sin^2\varphi$ is replaced by a suitable polarization factor.

2.1.4.2. Scattering by a system of two electrons

This can be derived along classical lines by calculating the phase difference between the X-ray beams scattered by each of the two electrons. A derivation based on quantum mechanics leads exactly to the same result by calculating the transition probability for the scattering of a primary quantum $(h\nu)_o$, given a secondary quantum $h\nu$ (Heitler, 1966, p. 193). For simplification we shall give only the classical derivation here. In Fig. 2.1.4.2, a system of two electrons is drawn with the origin at electron 1 and electron 2 at position **r**. They scatter the incident beam in a direction given by the vector **s**. The direction of the incident beam is along the vector $\mathbf{s}_o$. The length of the vectors can be chosen arbitrarily, but for convenience they are given a length $1/\lambda$. The two electrons scatter completely independently of each other.

Therefore, the amplitudes of the scattered beams 1 and 2 are equal, but they have a phase difference resulting from the path difference between the beam passing through electron 2 and the beam passing through electron 1. The path difference is $p + q = \lambda[\mathbf{r} \cdot (\mathbf{s}_o - \mathbf{s})]$. Beam 2 lags behind in phase compared with beam 1, and with respect to wave 1 its phase angle is

$$-2\pi\lambda[\mathbf{r} \cdot (\mathbf{s}_o - \mathbf{s})]/\lambda = 2\pi\mathbf{r} \cdot \mathbf{S}, \qquad (2.1.4.2)$$

where $\mathbf{S} = \mathbf{s} - \mathbf{s}_o$.

From Fig. 2.1.4.3, it is clear that the direction of **S** is perpendicular to an imaginary plane reflecting the incident beam at an angle θ and that the length of **S** is given by

$$|\mathbf{S}| = 2\sin\theta/\lambda. \qquad (2.1.4.3)$$

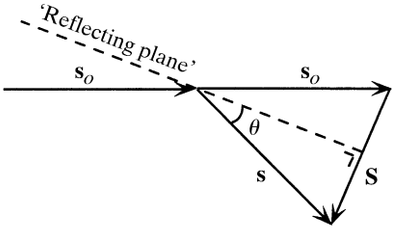

Figure 2.1.4.3
The direction of the incident wave is indicated by $\mathbf{s}_o$ and that of the scattered wave by **s**. Both vectors are of length $1/\lambda$. A plane that makes equal angles with **s** and $\mathbf{s}_o$ can be regarded as a mirror reflecting the incident beam. Reproduced with permission from Drenth (1999). Copyright (1999) Springer-Verlag.

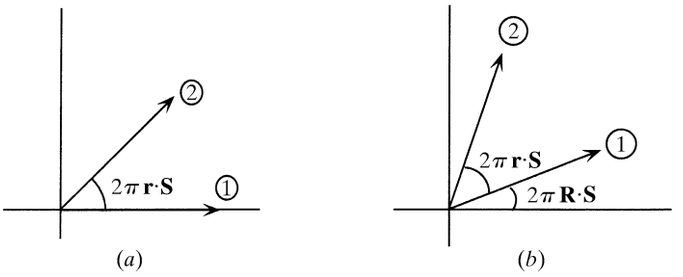

Figure 2.1.4.4
An Argand diagram for the scattering by two electrons. In (*a*), the origin is at electron 1; electron 2 is at position **r** with respect to electron 1. In (*b*), electron 1 is at position **R** with respect to the new origin, and electron 2 is at position $\mathbf{R} + \mathbf{r}$.

The total scattering from the two-electron system is $1 + 1 \times \exp(2\pi i\mathbf{r}\cdot\mathbf{S})$ if the resultant amplitude of the waves from electrons 1 and 2 is set to 1. In an Argand diagram, the waves are represented by vectors in a two-dimensional plane, as in Fig. 2.1.4.4(*a*).[1] Thus far, the origin of the system was chosen at electron 1. Moving the origin to another position simply means an equal change of phase angle for all waves. Neither the amplitudes nor the intensities of the reflected beams change (Fig. 2.1.4.4*b*).

2.1.4.3. Scattering by atoms

2.1.4.3.1. Scattering by one atom

Electrons in an atom are bound by the nucleus and are – in principle – not free electrons.

However, to a good approximation, they can be regarded as such if the frequency of the incident radiation ν is greater than the natural absorption frequencies, ν_n, at the absorption edges of the scattering atom, or the wavelength of the incident radiation is shorter than the absorption-edge wavelength (Section 2.1.4.4). This is normally true for light atoms but not for heavy ones (Table 2.1.4.1).

If the electrons in an atom can be regarded as free electrons, the scattering amplitude of the atom is a real quantity, because the electron cloud has a centrosymmetric distribution, *i.e.* $\rho(\mathbf{r}) = \rho(-\mathbf{r})$.

A small volume, $\mathrm{d}v_r$, at **r** contains $\rho(\mathbf{r}) \times \mathrm{d}v_r$ electrons, and at $-\mathbf{r}$ there are $\rho(-\mathbf{r}) \times \mathrm{d}v_r$ electrons. The combined scattering of the two volume elements, in units of the scattering of a free electron, is

$$\rho(\mathbf{r})\mathrm{d}v_r\{\exp(2\pi i\mathbf{r}\cdot\mathbf{S}) + \exp[2\pi i(-\mathbf{r})\cdot\mathbf{S}]\} = 2\rho(\mathbf{r})\cos(2\pi\mathbf{r}\cdot\mathbf{S})\mathrm{d}v_r;$$

this is a real quantity.

The scattering amplitude of an atom is called the atomic scattering factor *f*. It expresses the scattering of an atom in terms of the scattering of a single electron. *f* values are calculated for spherically averaged electron-density distributions and, therefore, do not depend on the scattering direction. They are tabulated in *IT* C (2004) as a function of $\sin\theta/\lambda$. The *f* values decrease appreciably as a function of $\sin\theta/\lambda$ (Fig. 2.1.4.5). This is due to interference effects between the scattering from the electrons in the cloud. In the direction $\theta = 0$, all electrons scatter in phase and the atomic scattering factor is equal to the number of electrons in the atom.

[1] The plane is also called the 'imaginary plane'. The real part of the vector in an Argand diagram is along the horizontal or real axis; the imaginary part is along the vertical or imaginary axis. Note also that $\exp(2\pi i\mathbf{r}\cdot\mathbf{S}) = \cos(2\pi\mathbf{r}\cdot\mathbf{S}) + i\sin(2\pi\mathbf{r}\cdot\mathbf{S})$. The cosine term is the real component and the sine term is the imaginary component.

Table 2.1.4.1
The position of the $K\alpha$ edge of different elements

Atomic number	Element	$K\alpha$ edge (Å)
6	C	43.68
16	S	5.018
26	Fe	1.743
34	Se	0.980
78	Pt	0.158

2.1.4.3.2. Scattering by a plane of atoms

A plane of atoms reflects an X-ray beam with a phase retardation of $\pi/2$ with respect to the scattering by a single atom. The difference is caused by the difference in path length from source (*S*) to atom (*M*) to detector (*D*) for the different atoms in the plane (Fig. 2.1.4.6). Suppose the plane is infinitely large. The shortest connection between *S* and *D via* the plane is *S*–*M*–*D*. The plane containing *S*, *M* and *D* is perpendicular to the reflecting plane, and the lines *SM* and *MD* form equal angles with the reflecting plane. Moving outwards from atom *M* in the reflecting plane, to *P* for instance, the path length *S*–*P*–*D* is longer. At the edge of the first Fresnel zone, the path is $\lambda/2$ longer (Fig. 2.1.4.6). This edge is an ellipse with its centre at *M* and its major axis on the line of intersection between the plane *SMD* and the reflecting plane. Continuing outwards, many more elliptic Fresnel zones are formed. Clearly, the beams radiated by the many atoms in the plane interfere with each other. The situation is represented in the Argand diagram in Fig. 2.1.4.7. Successive Fresnel zones can be subdivided into an equal number of subzones. If the distribution of electrons is sufficiently homogeneous, it can be assumed that the subzones in one Fresnel zone give the same amplitude at *D*. Their phases are spaced at regular intervals and their vectors in the Argand diagram lie in a half circle. In the lower part of Fig. 2.1.4.7, this is illustrated for the first Fresnel zone. For the second Fresnel zone (upper part),

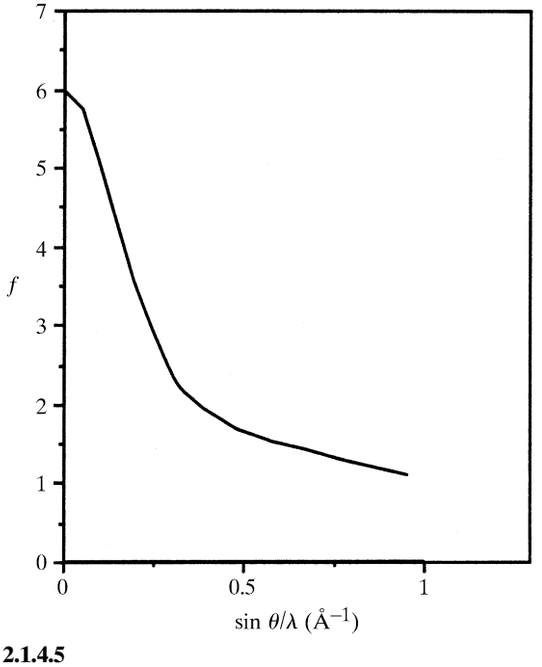

Figure 2.1.4.5
The atomic scattering factor *f* for carbon as a function of $\sin\theta/\lambda$, expressed in units of the scattering by one electron. Reproduced with permission from Drenth (1999). Copyright (1999) Springer-Verlag.

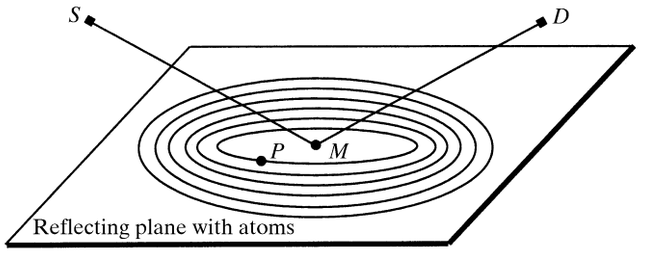

Figure 2.1.4.6
S is the X-ray source and *D* is the detector. The scattering is by the atoms in a plane. The shortest distance between *S* and *D via* a point in the plane is through *M*. Path lengths *via* points in the plane further out from *M* are longer, and when these beams reach the detector they lag behind in phase with respect to the *MD* beam. The plane is divided into zones, such that from one zone to the next the path difference is $\lambda/2$.

the radius is slightly smaller, because the intensity radiated by more distant zones decreases (Kauzmann, 1957). Therefore, the sum of vectors pointing upwards is shorter than that of those pointing downwards, and the resulting scattered wave lags $\pi/2$ in phase behind the scattering by the atom at *M*.

2.1.4.4. Anomalous dispersion

In classical dispersion theory, the scattering power of an atom is derived by supposing that the atom contains dipole oscillators. In units of the scattering of a free electron, the scattering of an oscillator with eigen frequency ν_n and moderate damping factor κ_n was found to be a complex quantity:

$$f_n = \nu^2/(\nu^2 - \nu_n^2 - i\kappa_n\nu), \qquad (2.1.4.4)$$

where ν is the frequency of the incident radiation [James, 1965; see also *IT* C (2004), equation (4.2.6.8)]. When $\nu \gg \nu_n$ in equation (2.1.4.4), f_n approaches unity, as is the case for scattering by a free electron; when $\nu \ll \nu_n$, f_n approaches zero, demonstrating the lack of scattering from a fixed electron. Only for $\nu \cong \nu_n$ does the imaginary part have an appreciable value.

Fortunately, quantum mechanics arrives at the same result by adding a rational meaning to the damping factors and interpreting ν_n as absorption frequencies of the atom (Hönl, 1933). For heavy atoms, the most important transitions are to a continuum of energy states, with $\nu_n \geq \nu_K$ or $\nu_n \geq \nu_L$ *etc.*, where ν_K and ν_L are the frequencies of the *K* and *L* absorption edges.

In practice, the complex atomic scattering factor, $f_{\text{anomalous}}$, is separated into three parts: $f_{\text{anomalous}} = f + f' + if''$. f is the contribution to the scattering if the electrons are free electrons and it is a real number (Section 2.1.4.3). f' is the real part of the correction to be applied and f'' is the imaginary correction; f'' is always $\pi/2$ in phase ahead of f (Fig. 2.1.4.8). $f + f'$ is the total real part of the atomic scattering factor.

The imaginary correction if'' is connected with absorption by oscillators having $\nu_n \cong \nu$. It can be calculated from the atomic absorption coefficient of the anomalously scattering element. For each of the *K*, *L etc.* absorption edges, f'' is virtually zero for frequencies below the edge, but it rises steeply at the edge and decreases gradually at higher frequencies.

The real correction f' can be derived from f'' by means of the Kramers–Kronig transform [*IT* C (2004), Section 4.2.6.2.2]. For frequencies close to an absorption edge, f' becomes strongly negative.

Values for f, f' and f'' are always given in units equal to the scattering by one free electron. f values are tabulated in *IT* C (2004) as a function of $\sin\theta/\lambda$, and the anomalous-scattering

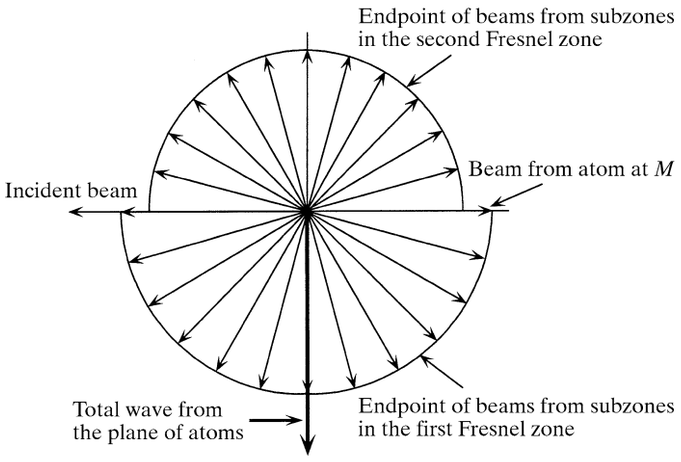

Figure 2.1.4.7
Schematic picture of the Argand diagram for the scattering by atoms in a plane. All electrons are considered free. The vector of the incident beam points to the left. The atom at *M* (see Fig. 2.1.4.6) has a phase difference of π with respect to the incident beam. Subzones in the first Fresnel zone have the endpoints of their vectors on the lower half circle. For the next Fresnel zone, they are on the upper half circle, which has a smaller radius because the amplitude decreases gradually for subsequent Fresnel zones (Kauzmann, 1957). The sum of all vectors points down, indicating a phase lag of $\pi/2$ with respect to the beam scattered by the atom at *M*.

corrections for forward scattering as a function of the wavelength. Because the anomalous contribution to the atomic scattering factor is mainly due to the electrons close to the nucleus, the value of the corrections diminishes much more slowly than f as a function of the scattering angle.

2.1.4.5. Scattering by a crystal

A unit cell contains a large number of electrons, especially in the case of biological macromolecules. The waves scattered by these electrons interfere with each other, thereby reducing the effective number of electrons in the scattered wave. The exception is scattering in the forward direction, where the beams from all electrons are in phase and add to each other. The effective number of scattering electrons is called the *structure factor F* because it depends on the structure, *i.e.* the distribution of the atoms in the unit cell. It also depends on the scattering direction. If small electron-density changes due to chemical bonding are neglected, the structure factor can be regarded as the sum of the scattering by the atoms in the unit cell, taking into consideration their positions and the corresponding phase differences between the scattered waves. For *n* atoms in the unit cell

$$F(\mathbf{S}) = \sum_{j=1}^{n} f_j \exp(2\pi i \mathbf{r}_j \cdot \mathbf{S}), \qquad (2.1.4.5)$$

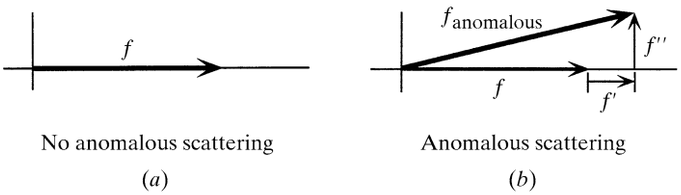

Figure 2.1.4.8
The atomic scattering factor as a vector in the Argand diagram. (*a*) When the electrons in the atom can be regarded as free. (*b*) When they are not completely free and the scattering becomes anomalous with a real anomalous contribution f' and an imaginary contribution if''. Reproduced with permission from Drenth (1999). Copyright (1999) Springer-Verlag.

where **S** is a vector perpendicular to the plane reflecting the incident beam at an angle θ; the length of **S** is given by $|\mathbf{S}| = 2\sin\theta/\lambda$ [equation (2.1.4.3) in Section 2.1.4.2].

The origin of the system is chosen at the origin of the selected unit cell. Atom j is at position $\mathbf{r}_j$ with respect to the origin. Another unit cell has its origin at $t \times \mathbf{a}$, $u \times \mathbf{b}$ and $v \times \mathbf{c}$, where t, u and v are whole numbers, and **a**, **b** and **c** are the basis vectors of the unit cell. With respect to the first origin, its scattering is

$$F(\mathbf{S})\exp(2\pi it\mathbf{a}\cdot\mathbf{S})\exp(2\pi iu\mathbf{b}\cdot\mathbf{S})\exp(2\pi iv\mathbf{c}\cdot\mathbf{S}).$$

The wave scattered by a crystal is the sum of the waves scattered by all unit cells. Assuming that the crystal has a very large number of unit cells ($n_1 \times n_2 \times n_3$), the amplitude of the wave scattered by the crystal is

$$W_{\rm cr}(\mathbf{S}) = F(\mathbf{S})\sum_{t=0}^{n_1}\exp(2\pi it\mathbf{a}\cdot\mathbf{S})\sum_{u=0}^{n_2}\exp(2\pi iu\mathbf{b}\cdot\mathbf{S}) \times \sum_{v=0}^{n_3}\exp(2\pi iv\mathbf{c}\cdot\mathbf{S}). \quad (2.1.4.6)$$

For an infinitely large crystal, the three summations over the exponential functions are delta functions. They have the property that they are zero unless

$$\mathbf{a}\cdot\mathbf{S} = h,\ \mathbf{b}\cdot\mathbf{S} = k \text{ and } \mathbf{c}\cdot\mathbf{S} = l, \quad (2.1.4.7)$$

where h, k and l are whole numbers, either positive, negative or zero. These are the Laue conditions. If they are fulfilled, all unit cells scatter in phase and *the amplitude of the wave scattered by the crystal is proportional to the amplitude of the structure factor F*. Its intensity is proportional to $|F|^2$.

S vectors satisfying equation (2.1.4.7) are denoted by **S**(hkl) or **S(h)**, and the corresponding structure factors as $F(hkl)$ or $F(\mathbf{h})$.

Bragg's law for scattering by a crystal is better known than the Laue conditions:

$$2d\sin\theta = \lambda, \quad (2.1.4.8)$$

where d is the distance between reflecting lattice planes, θ is the reflecting or glancing angle and λ is the wavelength (Fig. 2.1.4.9). It can easily be shown that the Laue conditions and Bragg's law are equivalent by combining equation (2.1.4.7) with the following information:

(1) Vector **S** is perpendicular to a reflecting plane (Section 2.1.4.2).

(2) The Laue conditions for scattering [equation (2.1.4.7)] can be written as

$$\frac{\mathbf{a}}{h}\cdot\mathbf{S} = 1;\quad \frac{\mathbf{b}}{k}\cdot\mathbf{S} = 1;\quad \frac{\mathbf{c}}{l}\cdot\mathbf{S} = 1. \quad (2.1.4.9)$$

(3) Lattice planes always divide the unit-cell vectors **a**, **b** and **c** into a number of equal parts (Section 2.1.1). If the lattice planes divide the **a** vector of the unit cell into h equal parts, the first index for this set of planes is h. The second index, k, is related to the division of **b** and the third index, l, to the division of **c**.

From equation (2.1.4.9) it follows that vector **S**(hkl) is perpendicular to a plane determined by the points **a**/h, **b**/k and **c**/l, and according to conditions (3) this is a lattice plane. Therefore, scattering by a crystal can indeed be regarded as reflection by lattice planes. The projection of **a**/h, **b**/k and **c**/l on vector **S**(hkl) is $1/|\mathbf{S}(hkl)|$ (Laue condition), but it is also equal to the spacing $d(hkl)$ between the lattice planes (see Fig. 2.1.1.3), and, therefore,

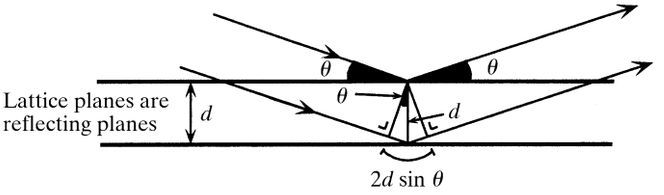

Figure 2.1.4.9
X-ray diffraction by a crystal is, in Bragg's conception, reflection by lattice planes. The beams reflected by successive planes have a path difference of $2d\sin\theta$, where d is the lattice-plane distance and θ is the reflecting angle. Positive interference occurs if $2d\sin\theta = \lambda, 2\lambda, 3\lambda$ *etc.*, where λ is the X-ray wavelength. Reproduced with permission from Drenth (1999). Copyright (1999) Springer-Verlag.

$|\mathbf{S}(hkl)| = 1/d(hkl)$. Combining this with equation (2.1.4.3) yields Bragg's law, $2d\sin\theta = \lambda$ [equation (2.1.4.8)].

2.1.4.6. The structure factor

For noncentrosymmetric structures, the structure factor,

$$F(\mathbf{S}) = \sum_{j=1}^{n} f_j \exp(2\pi i\mathbf{r}_j\cdot\mathbf{S}),$$

is an imaginary quantity and can also be written as[2]

$$F(\mathbf{S}) = \sum_{j=1}^{n} f_j\cos(2\pi\mathbf{r}_j\cdot\mathbf{S}) + i\sum_{j=1}^{n} f_j\sin(2\pi\mathbf{r}_j\cdot\mathbf{S}) = A(\mathbf{S}) + iB(\mathbf{S}).$$

It is sometimes convenient to split the structure factor into its real part, $A(\mathbf{S})$, and its imaginary part, $B(\mathbf{S})$. For centrosymmetric structures, $B(\mathbf{S}) = 0$ if the origin of the structure is chosen at the centre of symmetry.

The average value of the structure-factor amplitude $|F(\mathbf{S})|$ decreases with increasing $|\mathbf{S}|$ or, because $|\mathbf{S}| = 2\sin\theta/\lambda$, with increasing reflecting angle θ.

This is caused by two factors:

(1) A stronger negative interference between the electrons in the atoms at a larger scattering angle; this is expressed in the decrease of the atomic scattering factor as a function of **S**.

(2) The temperature-dependent vibrations of the atoms. Because of these vibrations, the apparent size of an atom is larger during an X-ray exposure, and the decrease in its scattering as a function of **S** is stronger. If the vibration is equally strong in all directions, it is called isotropic, and the atomic scattering factor must be multiplied by a correction factor, the temperature factor, $\exp[-B(\sin^2\theta)/\lambda^2]$. It can be shown that the parameter B is related to the mean-square displacement of the atomic vibrations, $\overline{u^2}$:

$$B = 8\pi^2\overline{u^2}.$$

In protein crystal structures determined at high resolution, each atom is given its own individual thermal parameter B.[3] Anisotropic thermal vibration is described by six parameters instead of one, and the evaluation of this anisotropic thermal vibration requires more data (X-ray intensities) than are usually available. Only at very high resolution (better than 1.5 Å) can one consider the incorporation of anisotropic temperature factors.

[2] For convenience, we write $F(\mathbf{S})$ when we mean $F(hkl)$ or $F(\mathbf{h})$, and **S** instead of **S**(hkl) or **S**(**h**).

[3] Do not confuse the thermal parameter B with the imaginary part $B(\mathbf{S})$ of the structure factor.

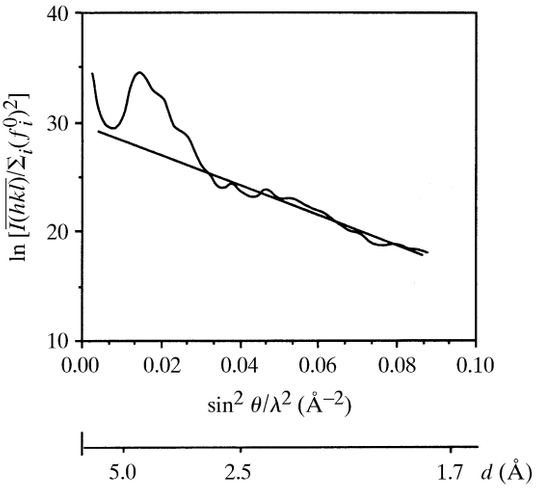

Figure 2.1.4.10
The Wilson plot for phospholipase A_2 with data to 1.7 Å resolution. Only beyond 3 Å resolution is it possible to fit the curve to a straight line. Reproduced with permission from Drenth (1999). Copyright (1999) Springer-Verlag.

The value of $|F(\mathbf{S})|$ can be regarded as the effective number of electrons per unit cell scattering in the direction corresponding to **S**. This is true if the values of $|F(\mathbf{S})|$ are on an absolute scale; this means that the unit of scattering is the scattering by one electron in a specific direction. The experimental values of $|F(\mathbf{S})|$ are normally on an arbitrary scale. The average value of the scattered intensity, $\overline{I(\text{abs.}, \mathbf{S})}$, on an absolute scale is $\overline{I(\text{abs.}, \mathbf{S})} = \overline{|F(\mathbf{S})|^2} = \sum_i f_i^2$, where f_i is the atomic scattering factor reduced by the temperature factor. This can be understood as follows:

$$I(\text{abs.}, \mathbf{S}) = F(\mathbf{S}) \cdot F^*(\mathbf{S}) = |F(\mathbf{S})|^2 = \sum_i \sum_j f_i f_j \exp\big[2\pi i(\mathbf{r}_i - \mathbf{r}_j) \cdot \mathbf{S}\big]. \quad (2.1.4.10)$$

For a large number of reflections, **S** varies considerably, and assuming that the angles $[2\pi(\mathbf{r}_i - \mathbf{r}_j) \cdot \mathbf{S}]$ are evenly distributed over the range 0–2π for $i \neq j$, the average value for the terms with $i \neq j$ will be zero and only the terms with $i = j$ remain, giving

$$\overline{|F(\mathbf{S})|^2} = \overline{I(\text{abs.}, \mathbf{S})} = \sum_i f_i^2. \quad (2.1.4.11)$$

Because of the thermal vibrations

$$f_i^2 = \exp\big(-2B_i \sin^2\theta/\lambda^2\big)(f_i^o)^2,$$

where i denotes a specific atom and f_i^o is the scattering factor for the atom i at rest.

It is sometimes necessary to transform the intensities and the structure factors from an arbitrary to an absolute scale. Wilson (1942) proposed a method for estimating the required scale factor K and, as an additional bonus, the thermal parameter B averaged over the atoms:

$$\overline{I(\mathbf{S})} = K\overline{I(\text{abs.}, \mathbf{S})} = K \exp(-2B \sin^2\theta/\lambda^2) \sum_i (f_i^o)^2. \quad (2.1.4.12)$$

To determine K and B, equation (2.1.4.11) is written in the form

$$\ln[\overline{I(\mathbf{S})}/\sum_i (f_i^o)^2] = \ln K - 2B \sin^2\theta/\lambda^2. \quad (2.1.4.13)$$

Because f_i^o depends on $\sin\theta/\lambda$, average intensities, $\overline{I(\mathbf{S})}$, are calculated for shells of narrow $\sin\theta/\lambda$ ranges. $\ln[\overline{I(\mathbf{S})}/\sum_i (f_i^o)^2]$ is plotted against $\sin^2\theta/\lambda^2$. The result should be a straight line with slope $-2B$, intersecting the vertical axis at $\ln K$ (Fig. 2.1.4.10).

For proteins, the Wilson plot gives rather poor results because the assumption in deriving equation (2.1.4.11) that the angles, $[2\pi(\mathbf{r}_i - \mathbf{r}_j) \cdot \mathbf{S}]$, are evenly distributed over the range 0–2π for $i \neq j$ is not quite valid, especially not in the $\sin\theta/\lambda$ ranges at low resolution.

As discussed above, the average value of the structure factors, $F(\mathbf{S})$, decreases with the scattering angle because of two effects:

(1) the decrease in the atomic scattering factor f;
(2) the temperature factor.

This decrease is disturbing for statistical studies of structure-factor amplitudes. It is then an advantage to eliminate these effects by working with normalized structure factors, $E(\mathbf{S})$, defined by

$$E(\mathbf{S}) = F(\mathbf{S}) \Big/ \left(\sum_j f_j^2\right)^{1/2} = F(\mathbf{S}) \exp\big(B \sin^2\theta/\lambda^2\big) \Big/ \left[\sum_j (f_j^o)^2\right]^{1/2}. \quad (2.1.4.14)$$

The application of equation (2.1.4.14) to $\overline{|E(\mathbf{S})|^2}$ gives

$$\overline{|E(\mathbf{S})|^2} = \overline{|F(\mathbf{S})|^2} \Big/ \sum_j f_j^2 = \overline{|F(\mathbf{S})|^2} \Big/ \overline{|F(\mathbf{S})|^2} = 1. \quad (2.1.4.15)$$

The average value, $\overline{|E(\mathbf{S})|^2}$, is equal to 1. The advantage of working with normalized structure factors is that the scaling is not important, because if equation (2.1.4.14) is written as

$$E(\mathbf{S}) = \frac{F(\mathbf{S})}{(\overline{|F(\mathbf{S})|^2})^{1/2}},$$

a scale factor affects numerator and denominator equally.

In practice, the normalized structure factors are derived from the observed data as follows:

$$E(\mathbf{S}) = F(\mathbf{S}) \exp\big(B \sin^2\theta/\lambda^2\big) \Big/ \big(\varepsilon |F(\mathbf{S})|^2\big)^{1/2}, \quad (2.1.4.16)$$

where ε is a correction factor for space-group symmetry. For general reflections it is 1, but it is greater than 1 for reflections having **h** parallel to a symmetry element. This can be understood as follows. For example, if m atoms are related by this symmetry element, $\mathbf{r}_j \cdot \mathbf{S}$ (with j from 1 to m) is the same in their contribution to the structure factor

$$F(\mathbf{h}) = \sum_{j=1}^{m} f_j \exp(2\pi i \mathbf{r}_j \cdot \mathbf{S}).$$

They act as one atom with scattering factor $m \times f$ rather than as m different atoms, each with scattering factor f. According to equation (2.1.4.11), this increases $F(\mathbf{h})$ by a factor $m^{1/2}$ on average. To make the F values of all reflections statistically comparable, $F(\mathbf{h})$ must be divided by $m^{1/2}$. For a detailed discussion, see *IT* B (2008), Chapter 2.1, by U. Shmueli and A. J. C. Wilson.

2.1.5. Reciprocal space and the Ewald sphere

A most convenient tool in X-ray crystallography is the reciprocal lattice. Unlike real or direct space, reciprocal space is imaginary. The reciprocal lattice is a superior instrument for constructing the X-ray diffraction pattern, and it will be introduced in the following way. Remember that vector $\mathbf{S}(hkl)$ is perpendicular to a reflecting plane and has a length $|\mathbf{S}(hkl)| = 2\sin\theta/\lambda = 1/d(hkl)$ (Section 2.1.4.5). This will now be applied to the boundary planes

of the unit cell: the *bc* plane or (100), the *ac* plane or (010) and the *ab* plane or (001).

For the *bc* plane or (100): indices $h = 1$, $k = 0$ and $l = 0$; $\mathbf{S}(100)$ is normal to this plane and has a length $1/d(100)$. Vector $\mathbf{S}(100)$ will be called $\mathbf{a}^*$.

For the *ac* plane or (010): indices $h = 0$, $k = 1$ and $l = 0$; $\mathbf{S}(010)$ is normal to this plane and has a length $1/d(010)$. Vector $\mathbf{S}(010)$ will be called $\mathbf{b}^*$.

For the *ab* plane or (001): indices $h = 0$, $k = 0$ and $l = 1$; $\mathbf{S}(001)$ is normal to this plane and has a length $1/d(001)$. Vector $\mathbf{S}(001)$ will be called $\mathbf{c}^*$.

From the definition of $\mathbf{a}^*$, $\mathbf{b}^*$ and $\mathbf{c}^*$ and the Laue conditions [equation (2.1.4.7)], the following properties of the vectors $\mathbf{a}^*$, $\mathbf{b}^*$ and $\mathbf{c}^*$ can be derived:

$$\mathbf{a}^* \cdot \mathbf{a} = \mathbf{a} \cdot \mathbf{a}^* = \mathbf{a} \cdot \mathbf{S}(100) = h = 1.$$

Similarly

$$\mathbf{b}^* \cdot \mathbf{b} = \mathbf{b} \cdot \mathbf{S}(010) = k = 1,$$

and

$$\mathbf{c}^* \cdot \mathbf{c} = \mathbf{c} \cdot \mathbf{S}(001) = l = 1.$$

However, $\mathbf{a}^* \cdot \mathbf{b} = 0$ and $\mathbf{a}^* \cdot \mathbf{c} = 0$ because $\mathbf{a}^*$ is perpendicular to the (100) plane, which contains the *b* and *c* axes. Correspondingly, $\mathbf{b}^* \cdot \mathbf{a} = \mathbf{b}^* \cdot \mathbf{c} = 0$ and $\mathbf{c}^* \cdot \mathbf{a} = \mathbf{c}^* \cdot \mathbf{b} = 0$.

Proposition. The endpoints of the vectors $\mathbf{S}(hkl)$ form the points of a lattice constructed with the unit vectors $\mathbf{a}^*$, $\mathbf{b}^*$ and $\mathbf{c}^*$.

Proof. Vector $\mathbf{S}$ can be split into its coordinates along the three directions a^*, b^* and c^*:

$$\mathbf{S} = X \cdot \mathbf{a}^* + Y \cdot \mathbf{b}^* + Z \cdot \mathbf{c}^*. \qquad (2.1.5.1)$$

Our proposition is true if X, Y and Z are whole numbers and indeed they are. Multiply equation (2.1.5.1) on the left and right side by $\mathbf{a}$.

$$\begin{array}{cccccc} \mathbf{a} \cdot \mathbf{S} = & X \cdot \mathbf{a} \cdot \mathbf{a}^* & + & Y \cdot \mathbf{a} \cdot \mathbf{b}^* & + & Z \cdot \mathbf{a} \cdot \mathbf{c}^* \\ \vdots & \vdots & & \vdots & & \vdots \\ = h & = X \cdot 1 & & = 0 & & = 0. \end{array}$$

The conclusion is that $X = h$, $Y = k$ and $Z = l$, and, therefore,

$$\mathbf{S} = h \cdot \mathbf{a}^* + k \cdot \mathbf{b}^* + l \cdot \mathbf{c}^*.$$

The diffraction by a crystal [equation (2.1.4.6)] is only different from zero if the Laue conditions [equation (2.1.4.7)] are satisfied. All vectors $\mathbf{S}(hkl)$ are vectors in reciprocal space ending in reciprocal-lattice points and not in between. Each vector $\mathbf{S}(hkl)$ is normal to the set of planes (hkl) in real space and has a length $1/d(hkl)$ (Fig. 2.1.5.1).

The reciprocal-lattice concept is most useful in constructing the directions of diffraction. The procedure is as follows:

Step 1: Draw the vector $\mathbf{s}_o$ indicating the direction of the incident beam from a point *M* to the origin, *O*, of the reciprocal lattice. As in Section 2.1.4.2, the length of $\mathbf{s}_o$ and thus the distance *MO* is $1/\lambda$ (Fig. 2.1.5.2).

Step 2: Construct a sphere with radius $1/\lambda$ and centre *M*. The sphere is called the Ewald sphere. The scattering object is thought to be placed at *M*.

Step 3: Move a reciprocal-lattice point *P* to the surface of the sphere. Reflection occurs with $\mathbf{s} = \mathbf{MP}$ as the reflected beam, but only if the reciprocal-lattice point *P* is on the surface of the sphere, because only then does $\mathbf{S}(hkl) = \mathbf{s} - \mathbf{s}_o$ (Section 2.1.4.2).

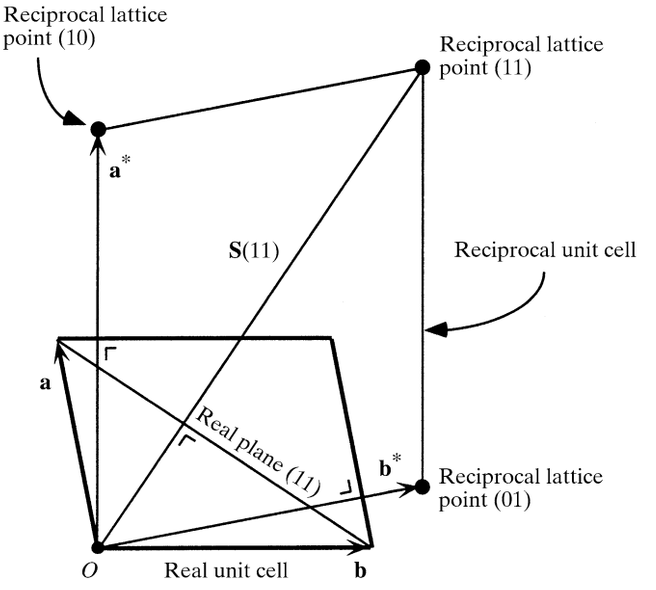

Figure 2.1.5.1
A two-dimensional real unit cell is drawn together with its reciprocal unit cell. The reciprocal-lattice points are the endpoints of the vectors $\mathbf{S}(hk)$ [in three dimensions $\mathbf{S}(hkl)$]; for instance, vector $\mathbf{S}(11)$ starts at *O* and ends at reciprocal-lattice point (11). Reproduced with permission from Drenth (1999). Copyright (1999) Springer-Verlag.

Noncrystalline objects scatter differently. Their scattered waves are not restricted to reciprocal-lattice points passing through the Ewald sphere. They scatter in all directions.

2.1.6. Mosaicity and integrated reflection intensity

Crystals hardly ever have a perfect arrangement of their molecules, and crystals of macromolecules are certainly not perfect. Their crystal lattices show defects, which can sometimes be observed with an atomic force microscope or by interferometry. A schematic but useful way of looking at non-perfect crystals is through mosaicity; the crystal consists of a large number of tiny blocks. Each block is regarded as a perfect crystal, but the blocks are slightly misaligned with respect to each other. Scattering from different blocks is incoherent. Mosaicity causes a spread in the diffracted beams; when combined with the divergence of the beam from the X-ray source, this is called the effective mosaic spread. For the same crystal, effective mosaicity is smaller in a synchrotron beam with its lower divergence than in the laboratory. Protein crystals usually show a mosaic spread of 0.25–0.5°. Mosaic spread increases due to distortion of the lattice; this can happen as a result of flash freezing or radiation damage, for instance.

In Section 2.1.4.5, it was stated that the amplitude of the wave scattered by a crystal is proportional to the structure-factor amplitude $|F|$ and that its intensity is proportional to $|F|^2$. Of course, other factors also determine the intensity of the scattered beam, such as the wavelength, the intensity of the incident beam, the volume of the crystal *etc*. The intensity integrated over the entire region of the diffraction spot *hkl* is

$$I_{\rm int}(hkl) = \frac{\lambda^3}{\omega V^2}\left(\frac{e^2}{mc^2}\right)^2 V_{\rm cr} I_o LPT |F(hkl)|^2. \qquad (2.1.6.1)$$

In equation (2.1.6.1), we recognize $I_o(e^2/mc^2)^2$ as part of the Thomson scattering for one electron, $I_{\rm el} = I_o(e^2/mc^2)^2 \sin^2\varphi$ [equations (2.1.4.1*a*) and (2.1.4.1*b*)] per unit solid angle. $V_{\rm cr}$ is the

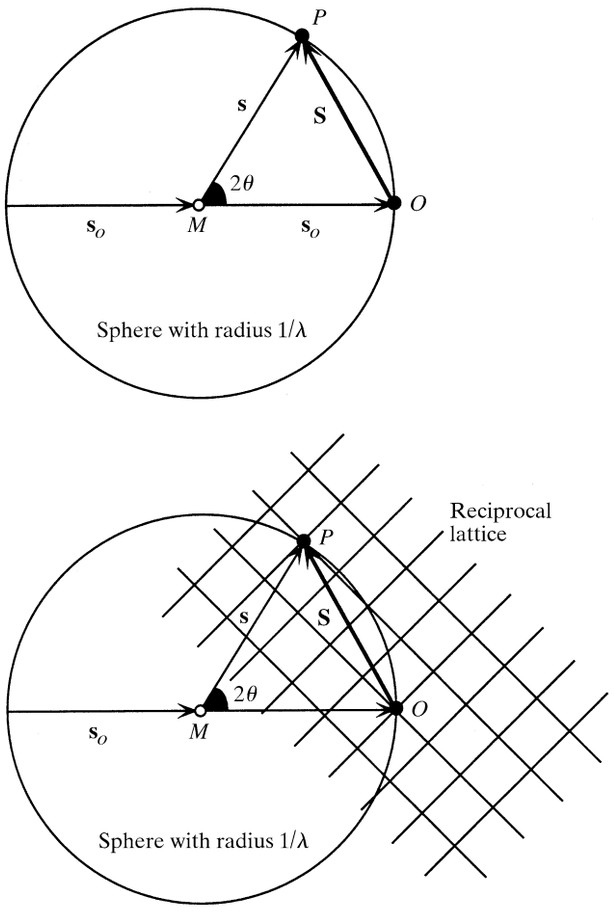

Figure 2.1.5.2
The circle is, in fact, a sphere with radius $1/\lambda$. $\mathbf{s}_O$ indicates the direction of the incident beam and has a length $1/\lambda$. The diffracted beam is indicated by vector $\mathbf{s}$, which also has a length $1/\lambda$. Only reciprocal-lattice points on the surface of the sphere are in a reflecting position. Reproduced with permission from Drenth (1999). Copyright (1999) Springer-Verlag.

volume of the crystal and V is the volume of the unit cell. It is clear that the scattered intensity is proportional to the volume of the crystal. The term $1/V^2$ can be explained as follows. In a mosaic block, all unit cells scatter in phase. For a given volume of the individual blocks, the number of unit cells in a mosaic block, as well as the scattering amplitude, is proportional to $1/V$. The scattered intensity is then proportional to $1/V^2$. Because of the finite reflection width, scattering occurs not only for the reciprocal-lattice point when it is on the Ewald sphere, but also for a small volume around it. Since the sphere has radius $1/\lambda$, the solid angle for scattering, and thus the intensity, is proportional to $1/(1/\lambda)^2 = \lambda^2$.

However, in equation (2.1.6.1), the scattered intensity is proportional to λ^3. The extra λ dependence is related to the time t it takes for the reciprocal-lattice 'point' to pass through the surface of the Ewald sphere. With an angular speed of rotation ω, a reciprocal-lattice point at a distance $1/d$ from the origin of the reciprocal lattice moves with a linear speed $v = (1/d)\omega$ if the rotation axis is normal to the plane containing the incident and reflected beam. For the actual passage through the surface of the Ewald sphere, the component perpendicular to the surface is needed: $v_\perp = (1/d)\omega\cos\theta = \omega\sin 2\theta/\lambda$. Therefore, the time t required to pass through the surface is proportional to $(1/\omega)(\lambda/\sin 2\theta)$. This introduces the extra λ term in equation (2.1.6.1) as well as the ω dependence and a $1/\sin 2\theta$ term. The latter represents the Lorentz factor L. It is a geometric correction factor for the hkl reflections; here it is $1/\sin 2\theta$, but it is different for other data-collection geometries.

The factor P in equation (2.1.6.1) is the polarization factor. For the polarized incident beam used in deriving equation (2.1.4.1*a*), $P = \sin^2\varphi$, where φ is the angle between the polarization direction of the beam and the scattering direction. It is easy to verify that $\phi = 90^\circ - 2\theta$, where θ is the reflecting angle (Fig. 2.1.4.9). P depends on the degree of polarization of the incident beam. For a completely unpolarized beam, $P = (1 + \cos^2 2\theta)/2$.

In equation (2.1.6.1), T is the transmission factor: $T = 1 - A$, where A is the absorption factor. When X-rays travel through matter, they suffer absorption. The overall absorption follows Beer's law:

$$I = I_o \exp(-\mu d),$$

where I_o is the intensity of the incident beam, d is the path length in the material and μ is the total linear absorption coefficient. μ can be obtained as the sum of the atomic mass absorption coefficients of the elements $(\mu_m)_i$:

$$\mu = \rho \sum_i g_i(\mu_m)_i,$$

where ρ is the density of the absorbing material and g_i is the mass fraction of element i.

Atomic mass absorption coefficients $(\mu_m)_i$ for the elements are listed in Tables 4.2.4.3 (and 4.2.4.1) of *IT* C (2004) as a function of a large number of wavelengths. The absorption is wavelength-dependent and is generally much stronger for longer wavelengths. This is the result of several processes. For the X-ray wavelengths applied in crystallography, the processes are scattering and photoelectric absorption. Moreover, at the reflection position, the intensity may be reduced by extinction.

Scattering is the result of a collision between the X-ray photons and the electrons. One can distinguish two kinds of scattering: Compton scattering and Rayleigh scattering. In Compton scattering, the photons lose part of their energy in the collision process (inelastic scattering), resulting in scattered photons with a lower energy and a longer wavelength. Compton scattering contributes to the background in an X-ray diffraction experiment. In Rayleigh scattering, the photons are elastically scattered, do not lose energy, and leave the material with their wavelength unchanged. In a crystal, they interfere with each other and give rise to the Bragg reflections. Between the Bragg reflections, there is no loss of energy due to elastic scattering and the incident beam is hardly reduced. In the Bragg positions, if the reduction in intensity of the incident beam due to elastic scattering can still be neglected, the crystal is considered an ideal mosaic. For non-ideal mosaic crystals, the beam intensity is reduced by *extinction*:

(1) The blocks are too large, and multiple reflection occurs within a block. At each reflection process, the phase angle shifts $\pi/2$ (Section 2.1.4.3.2). After two reflections, the beam travels in the same direction as the incident beam but with a phase difference of π, and this reduces the intensity.
(2) The angular spread of the blocks is too small. The incident beam is partly reflected by blocks close to the surface and the resulting beam is the incident beam for the lower-lying blocks that are also in reflecting position.

Extinction is not a serious problem in protein X-ray crystallography.

Absorption curves as a function of the X-ray wavelength show anomalies at absorption edges. At such an edge, electrons are

ejected from the atom or are elevated to a higher-energy bound state, the photons disappear completely and the X-ray beam is strongly absorbed. This is called *photoelectric absorption*. At an absorption edge, the frequency of the X-ray beam ν is equal to the frequency ν_K, ν_L or ν_M corresponding to the energy of the K, L or M state. According to equation (2.1.4.4), anomalous scattering is maximal at an absorption edge.

2.1.7. Calculation of electron density

In equation (2.1.4.6), the wave $W_{\rm cr}(\mathbf{S})$ scattered by the crystal is given as the sum of the atomic contributions, as in equation (2.1.4.5) for the scattering by a unit cell. In the derivation of equation (2.1.4.5), it is assumed that the atoms are spherically symmetric (Section 2.1.4.3) and that density changes due to chemical bonding are neglected. A more exact expression for the wave scattered by a crystal, in the absence of anomalous scattering, is

$$W_{\rm cr}(\mathbf{S}) = \int_{\rm crystal} \rho(\mathbf{r}) \exp(2\pi i \mathbf{r}\cdot\mathbf{S})\ {\rm d}v_{\rm real}. \qquad (2.1.7.1)$$

The integration is over all electrons in the crystal. $\rho(\mathbf{r})$ is the electron-density distribution in each unit cell. The operation on the electron-density distribution in equation (2.1.7.1) is called Fourier transformation, and $W_{\rm cr}(\mathbf{S})$ is the Fourier transform of $\rho(\mathbf{r})$. It can be shown that $\rho(\mathbf{r})$ is obtained by an inverse Fourier transformation:

$$\rho(\mathbf{r}) = \int_{\mathbf{S}} W_{\rm cr}(\mathbf{S}) \exp(-2\pi i \mathbf{r}\cdot\mathbf{S})\ {\rm d}v_{\rm reciprocal}. \qquad (2.1.7.2)$$

In contrast to $\rho(\mathbf{r})$, $W_{\rm cr}(\mathbf{S})$ is not a continuous function but, because of the Laue conditions, it is only different from zero at the reciprocal-lattice points $\mathbf{h}\ (= hkl)$. In equation (2.1.4.6), $W_{\rm cr}(\mathbf{S})$ is the product of the structure factor and three delta functions. The structure factor at the reciprocal-lattice points is $F(\mathbf{h})$, and the product of the three delta functions is $1/V$, the volume of one reciprocal unit cell. Therefore, $W_{\rm cr}(\mathbf{S})$ in equation (2.1.7.2) can be replaced by $F(\mathbf{h})/V$, and equation (2.1.7.2) itself by

$$\rho(\mathbf{r}) = (1/V) \sum_{\mathbf{h}} F(\mathbf{h}) \exp(-2\pi i \mathbf{r}\cdot\mathbf{h}). \qquad (2.1.7.3)$$

If x, y and z are fractional coordinates in the unit cell, $\mathbf{r}\cdot\mathbf{S} = (\mathbf{a}\cdot x + \mathbf{b}\cdot y + \mathbf{c}\cdot z)\cdot\mathbf{S} = \mathbf{a}\cdot\mathbf{S}\cdot x + \mathbf{b}\cdot\mathbf{S}\cdot y + \mathbf{c}\cdot\mathbf{S}\cdot z = hx + ky + lz$, and an alternative expression for the electron density is

$$\rho(xyz) = (1/V) \sum_h \sum_k \sum_l F(hkl) \exp[-2\pi i(hx + ky + lz)]. \qquad (2.1.7.4)$$

Instead of expressing $F(\mathbf{S})$ as a summation over the atoms [equation (2.1.4.5)], it can be expressed as an integration over the electron density in the unit cell:

$$F(hkl) = V \int_{x=0}^{1} \int_{y=0}^{1} \int_{z=0}^{1} \rho(xyz) \exp[2\pi i(hx + ky + lz)]\ {\rm d}x\ {\rm d}y\ {\rm d}z. \qquad (2.1.7.5)$$

Because $F(hkl)$ is a vector in the Argand diagram with an amplitude $|F(hkl)|$ and a phase angle $\alpha(hkl)$,

$$F(hkl) = |F(hkl)| \exp[i\alpha(hkl)]$$

and

$$\rho(xyz) = (1/V) \sum_h \sum_k \sum_l |F(hkl)| \exp[-2\pi i(hx + ky + lz) + i\alpha(hkl)]. \qquad (2.1.7.6)$$

By applying equation (2.1.7.6), the electron-density distribution in the unit cell can be calculated, provided values of $|F(hkl)|$ and $\alpha(hkl)$ are known. From equation (2.1.6.1), it is clear that $|F(hkl)|$ can be derived, on a relative scale, from $I_{\rm int}(hkl)$ after a correction for the background and absorption, and after application of the Lorentz and polarization factor:

$$|F(hkl)| = \left[\frac{I_{\rm int}(hkl)}{LPT}\right]^{1/2}. \qquad (2.1.7.7)$$

Contrary to the situation with crystals of small compounds, it is not easy to find the phase angles $\alpha(hkl)$ for crystals of macromolecules by direct methods, although these methods are in a state of development (see Part 16). Indirect methods to determine the protein phase angles are:

(1) isomorphous replacement (see Part 12);
(2) molecular replacement (see Part 13);
(3) multiple-wavelength anomalous dispersion (MAD) (see Part 14).

From equation (2.1.7.5), it is clear that the reflections hkl and $\overline{hkl}$ have the same value for their structure-factor amplitudes, $|F(hkl)| = |F(\overline{hkl})|$, and for their intensities, $I(hkl) = I(\overline{hkl})$, but have opposite values for their phase angles, $\alpha(hkl) = -\alpha(\overline{hkl})$, assuming that anomalous dispersion can be neglected. Consequently, equation (2.1.7.6) reduces to

$$\rho(xyz) = (1/V) \sum_h \sum_k \sum_l |F(hkl)| \cos[2\pi(hx + ky + lz) - \alpha(hkl)] \qquad (2.1.7.8)$$

or

$$\rho(xyz) = F(000)/V + (2/V) \sum_h{}' \sum_k{}' \sum_l{}' |F(hkl)| \times \cos[2\pi(hx + ky + lz) - \alpha(hkl)]. \qquad (2.1.7.9)$$

$\sum'$ denotes that $F(000)$ is excluded from the summation and that only the reflections hkl, and not $\overline{hkl}$, are considered.

The two reflections, hkl and $\overline{hkl}$, are called Friedel or Bijvoet pairs.

If anomalous dispersion cannot be neglected, the two members of a Friedel pair have different values for their structure-factor amplitudes, and their phase angles no longer have opposite values. This is caused by the f'' contribution to the anomalous scattering (Fig. 2.1.7.1). Macromolecular crystals show anomalous dispersion if the structure contains, besides the light atoms, one or more heavier atoms. These can be present in the native structure or are introduced in the isomorphous replacement technique or in MAD analysis.

2.1.8. Symmetry in the diffraction pattern

In the previous section, it was noted that $I(hkl) = I(\overline{hkl})$ if anomalous scattering can be neglected. In this case, the effect is that the diffraction pattern has a centre of symmetry. This is also true for the reciprocal lattice if the reciprocal-lattice points (hkl) are weighted with their $I(hkl)$ values. If the crystal structure has symmetry elements, they are also found in the diffraction pattern and in the weighted reciprocal lattice. Macromolecular crystals of biological origin are enantiomorphic and the symmetry operators in the crystal are restricted to rotation axes and screw axes. It is evident that a rotation of the real lattice will cause the same

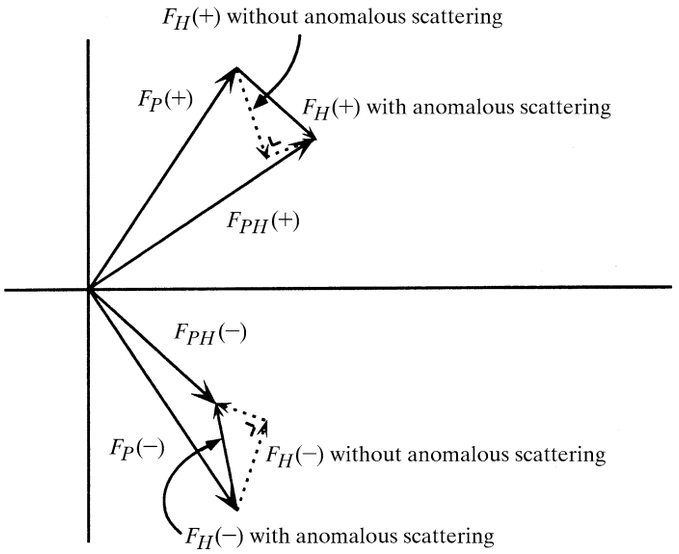

Figure 2.1.7.1
An Argand diagram for the structure factors of the two members of a Friedel pair. (+) represents *hkl* and (−) represents $\overline{hkl}$. F_P is the contribution to the structure factor by the non-anomalously scattering protein atoms and F_H is that for the anomalously scattering atoms. F_H consists of a real part with an imaginary part perpendicular to it. The real parts are mirror images with respect to the horizontal axis. The imaginary parts are rotated counterclockwise with respect to the real parts (Section 2.1.4.4). The result is that the total structure factors, $F_{PH}(+)$ and $F_{PH}(-)$, have different amplitudes and phase angles. Reproduced with permission from Drenth (1999). Copyright (1999) Springer-Verlag.

rotation of the reciprocal lattice. If this rotation is the result of a symmetry operation around an axis, the crystal structure looks exactly the same as before the rotation, and the same must be true for the weighted reciprocal lattice. However, screw axes in the crystal lattice reduce to normal (non-screw) rotation axes in the weighted reciprocal lattice, as has been shown by Waser (1955). We follow his arguments, but must first introduce matrix notation for convenience.

If $\mathbf{r}$ is a position vector and $\mathbf{h}$ a vector in reciprocal space, the scalar product

$$\mathbf{h}\cdot\mathbf{r} = (h\mathbf{a}^* + k\mathbf{b}^* + l\mathbf{c}^*)\cdot(\mathbf{a}x + \mathbf{b}y + \mathbf{c}z) = hx + ky + lz,$$

or in matrix notation,

$$(hkl)\begin{pmatrix} x \\ y \\ z \end{pmatrix} = \mathbf{h}^T\mathbf{r},$$

where $(hkl) = \mathbf{h}^T$ is a row vector and

$$\begin{pmatrix} x \\ y \\ z \end{pmatrix} = \mathbf{r}$$

is a column vector. $\mathbf{h}^T$ is the transpose of column vector $\mathbf{h}$ (rows and columns are interchanged). In this notation, the structure factor is given by

$$F(\mathbf{h}) = \int_{\text{cell}} \rho(\mathbf{r})\exp(2\pi i\mathbf{h}^T\cdot\mathbf{r})\ \mathrm{d}v_{\text{real}}. \qquad (2.1.8.1)$$

The symmetry operation of a screw axis is a combination of a rotation and a translation. The rotation can be represented by the matrix $\mathbf{R}$ and the translation by the vector $\mathbf{t}$. Because of the screw-axis symmetry, $\rho(\mathbf{R}\cdot\mathbf{r}+\mathbf{t}) = \rho(\mathbf{r})$.

$F(\mathbf{h})$ can also be expressed as

$$\begin{aligned} F(\mathbf{h}) &= \int_{\text{cell}} \rho(\mathbf{R}\cdot\mathbf{r}+\mathbf{t})\exp[2\pi i\mathbf{h}^T\cdot(\mathbf{R}\cdot\mathbf{r}+\mathbf{t})]\ \mathrm{d}v_{\text{real}} \\ &= \exp(2\pi i\mathbf{h}^T\cdot\mathbf{t})\int_{\text{cell}} \rho(\mathbf{r})\exp(2\pi i\mathbf{h}^T\cdot\mathbf{R}\cdot\mathbf{r})\ \mathrm{d}v_{\text{real}}. \qquad (2.1.8.2)\end{aligned}$$

Because $\mathbf{h}^T\cdot\mathbf{R} = (\mathbf{R}^T\cdot\mathbf{h})^T$, where $\mathbf{R}^T$ is the transpose of the matrix $\mathbf{R}$, equation (2.1.8.2) can be written as

$$F(\mathbf{h}) = \exp(2\pi i\mathbf{h}^T\cdot\mathbf{t})\int_{\text{cell}} \rho(\mathbf{r})\exp[2\pi i(\mathbf{R}^T\cdot\mathbf{h})^T\cdot\mathbf{r}]\ \mathrm{d}v_{\text{real}}. \qquad (2.1.8.3)$$

By definition, the integral in equation (2.1.8.3) is $F(\mathbf{R}^T\cdot\mathbf{h})$, and, therefore

$$F(\mathbf{h}) = \exp(2\pi i\mathbf{h}^T\cdot\mathbf{t})F(\mathbf{R}^T\cdot\mathbf{h}).$$

Conclusion: The phase angles of the two structure factors are different for $\mathbf{t}\neq 0$:

$$\alpha(\mathbf{h}) = \alpha(\mathbf{R}^T\cdot\mathbf{h}) + 2\pi\mathbf{h}^T\cdot\mathbf{t}, \qquad (2.1.8.4)$$

but the structure-factor amplitudes and, therefore, the intensities are always equal:

$$I(\mathbf{h}) = I(\mathbf{R}^T\cdot\mathbf{h}) \quad \text{or} \quad I[(\mathbf{R}^T)^{-1}\cdot\mathbf{h}] = I(\mathbf{h}). \qquad (2.1.8.5)$$

The matrices $(\mathbf{R}^T)^{-1}$ in reciprocal space and $\mathbf{R}$ in direct space denote rotation over the same angle. Therefore, both an *n*-fold screw axis and an *n*-fold rotation axis in the crystal correspond to an *n*-fold axis in the weighted reciprocal lattice.

However, screw axes distinguish themselves from non-screw axes by extinction of some reflections along the line in reciprocal space corresponding to the screw-axis direction. This will be shown for a twofold screw axis along the monoclinic *b* axis.

The electron density at $\mathbf{r}$, $\rho(\mathbf{r})$, is then equal to the electron density at $\mathbf{R}\cdot\mathbf{r}+\mathbf{t}$, where $\mathbf{R}\cdot\mathbf{r}$ is a rotation that leaves the value of the *y* coordinate unchanged. $\mathbf{t}$ is equal to $\mathbf{b}/2$.

$$F(\mathbf{h}) = \int_{\text{half the cell}} \rho(\mathbf{r})\{\exp(2\pi i\mathbf{h}^T\cdot\mathbf{r}) + \exp[2\pi i\mathbf{h}^T(\mathbf{R}\cdot\mathbf{r}+\mathbf{t})]\}\ \mathrm{d}v_{\text{real}}. \qquad (2.1.8.6)$$

For the $(0k0)$ reflections, ($\mathbf{h}$ along $\mathbf{b}^*$) is $\mathbf{h} = k\mathbf{b}^*$, giving

$$\mathbf{h}^T\cdot\mathbf{r} = \mathbf{h}^T\cdot\mathbf{R}\cdot\mathbf{r} = 0 + ky + 0 \text{ and } \mathbf{h}^T\cdot\mathbf{t} = k/2.$$

This simplifies equation (2.1.8.6) to

$$F(0k0) = [1+\exp(\pi ik)]\int_{\text{half the cell}} \rho(\mathbf{r})\exp(2\pi iky)\ \mathrm{d}v_{\text{real}}. \qquad (2.1.8.7)$$

If k is odd, $F(0k0) = 0$, because $1+\exp(\pi ik) = 0$.

This type of systematic absence, due to screw components in the symmetry elements, occurs along lines in reciprocal space. Other types of absence apply to all *hkl* reflections. They result from the centring of the unit cell (Fig. 2.1.1.4). Suppose the unit cell is centred in the *ab* plane (*C* centring). Consequently, the electron density at $\mathbf{r}$ is equal to the electron density at $\mathbf{r}+\mathbf{t}$, with $\mathbf{t} = \mathbf{a}/2 + \mathbf{b}/2$ and $\mathbf{h}^T\cdot\mathbf{t} = h/2 + k/2$. The structure factor can then be written as

$$F(\mathbf{h}) = \{1+\exp[\pi i(h+k)]\}\int_{\text{half the cell}} \rho(\mathbf{r})\exp\left(2\pi i\mathbf{h}^T\cdot\mathbf{r}\right)\ \mathrm{d}v_{\text{real}}. \qquad (2.1.8.8)$$

The conclusion is that when $(h+k)$ is odd, the structure factors are zero and no diffracted intensity is observed for those reflections.

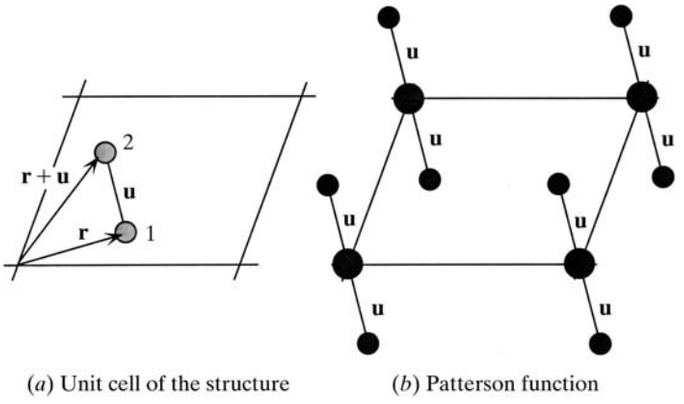

(*a*) Unit cell of the structure (*b*) Patterson function

Figure 2.1.9.1
(*a*) A two-dimensional unit cell with two atoms. (*b*) The corresponding Patterson function. Reproduced with permission from Drenth (1999). Copyright (1999) Springer-Verlag.

2.1.9. The Patterson function

In 1934, A. L. Patterson presented a method for locating the atomic positions in not too complicated molecules without knowledge of the phase angles (Patterson, 1934). The method involves the calculation of the Patterson function, $P(uvw) = P(\mathbf{u})$:

$$P(\mathbf{u}) = (1/V) \sum_{\mathbf{h}} |F(\mathbf{h})|^2 \cos(2\pi \mathbf{h} \cdot \mathbf{u}), \qquad (2.1.9.1)$$

or, written as an exponential function,

$$P(\mathbf{u}) = (1/V) \sum_{\mathbf{h}} |F(\mathbf{h})|^2 \exp(2\pi i \mathbf{h} \cdot \mathbf{u}). \qquad (2.1.9.2)$$

Equations (2.1.9.1) and (2.1.9.2) give the same result, because in the definition of $P(\mathbf{u})$ anomalous dispersion is neglected, resulting in $|F(\mathbf{h})|^2 = |F(-\mathbf{h})|^2$. Comparison with equations (2.1.7.3) and (2.1.7.6) shows that the Patterson function $P(\mathbf{u})$ is a Fourier summation with coefficients $|F(\mathbf{h})|^2$ instead of $F(\mathbf{h}) = |F(\mathbf{h})| \exp[i\alpha(\mathbf{h})]$. The periodicity, and thus the unit cell, are the same for the electron density and the Patterson function. For the Patterson function, many authors prefer to use $\mathbf{u}$ rather than $\mathbf{r}$ as the position vector.

The fundamental advantage of Patterson's discovery is that, in contrast to the calculation of $\rho(\mathbf{r})$, no phase information is needed for calculating $P(\mathbf{u})$.

The Patterson map can be obtained directly after the intensities of the reflections have been measured and corrected. However, what kind of information does it provide? This can be understood from an alternative expression for the Patterson function:

$$P(\mathbf{u}) = \int_{\mathbf{r}} \rho(\mathbf{r}) \rho(\mathbf{r} + \mathbf{u}) \, \mathrm{d}v_{\mathrm{real}}. \qquad (2.1.9.3)$$

Equation (2.1.9.3) leads to the same result as equation (2.1.9.1), as can be proved easily by substituting expression (2.1.7.3) for ρ in the right-hand side of equation (2.1.9.3).

On the right-hand side of the equation, the electron density $\rho(\mathbf{r})$ at position $\mathbf{r}$ in the unit cell is multiplied by the electron density $\rho(\mathbf{r} + \mathbf{u})$ at position $\mathbf{r} + \mathbf{u}$; the integration is over all vectors $\mathbf{r}$ in the unit cell. The result of the integration is that the Patterson map will show peaks at the end of vectors $\mathbf{u}$ between atoms in the unit cell of the structure; all these Patterson vectors start at the origin of the Patterson cell. This can best be understood with a simple example. In Fig. 2.1.9.1, a two-dimensional unit cell is drawn containing only two atoms (1 and 2). To calculate the Patterson map, a vector $\mathbf{u}$ must be moved through this cell, and, according to equation (2.1.9.3), for every position and orientation of $\mathbf{u}$, the electron densities at the beginning and at the end of $\mathbf{u}$ must be multiplied. It is clear that this product will generally be zero unless the length and the orientation of $\mathbf{u}$ are such that it begins in atom 1 and ends in atom 2, or the other way around. If so, there is a peak in the Patterson map at the end of vector $\mathbf{u}$ and at the end of vector $-\mathbf{u}$, implying that the Patterson map is always centrosymmetric. The origin itself, where vector $\mathbf{u} = 0$, always has a high peak because

$$P(\mathbf{u} = 0) = \int_{\mathbf{r}} \rho(\mathbf{r}) \rho(\mathbf{r}) \, \mathrm{d}v_{\mathrm{real}} = \sum_{\mathbf{h}} |F(\mathbf{h})|^2.$$

The origin peak is equal to the sum of the squared local electron densities. The height of each non-origin peak is proportional to the product of $\rho(\mathbf{r})$ and $\rho(\mathbf{r} + \mathbf{u})$. This is an important feature in the isomorphous replacement method for protein-structure determination, in which the heavy-atom positions are derived from a difference Patterson calculated with coefficients $(|F_{PH}| - |F_P|)^2$, where $|F_{PH}|$ is the structure-factor amplitude of the heavy-atom derivative and $|F_P|$ is that of the native protein (see Part 12). The vectors between the heavy atoms are the most prominent features in such a map.

The number of peaks in a Patterson map increases much faster than the number of atoms. For n atoms in the real unit cell, there are n^2 Patterson peaks, n of them superimposed at the origin, and $n \times (n - 1)$ elsewhere in the Patterson cell. Because the atomic electron densities cover a certain region and the width of a Patterson peak at $\mathbf{u}$ is roughly the sum of the widths of the atoms connected by $\mathbf{u}$, overlap of peaks is a real problem in the interpretation of a Patterson map. It can almost only be done for unit cells with a restricted number of atoms unless some extra information is available. For crystals of macromolecules, it is certainly impossible to derive the structure from an interpretation of the Patterson map.

The situation can be improved through sharpening the Patterson peaks by simulating the atoms as point scatterers. This can be achieved by replacing the $|F(\mathbf{h})|^2$ values with modified intensities which, on average, do not decrease with $\sin\theta/\lambda$. For instance, suitable intensities for this purpose are the squared normalized structure-factor amplitudes $|E(\mathbf{h})|^2$ (Section 2.1.4.6), the average of which is 1 at all $\sin\theta/\lambda$. A disadvantage of sharpening to point peaks is the occurrence of diffraction ripples around the sharp peaks, induced by truncation of the Fourier series in equation (2.1.9.1). Therefore, modified intensities corresponding to less sharpened peaks are sometimes used [*IT* B (2008), Chapter 2.3, pp. 245–246]. Diffraction ripples that seriously disturb the Patterson map are generated by the high origin peak, and, particularly for sharpened maps, it is advisable to remove this peak. This implies that $P(\mathbf{u} = 0) = 0$ [equation (2.1.9.1)]. It is easy to verify that this requires coefficients $[|F(\mathbf{h})|^2 - \langle |F(\mathbf{h})|^2 \rangle]$ for the $|F(\mathbf{h})|^2$ map and $[|E(\mathbf{h})|^2 - 1]$ for the $|E(\mathbf{h})|^2$ map. Note that the term for $\mathbf{h} = 0$ is omitted and that the average of $|F(\mathbf{h})|^2$ must be taken for the appropriate $\sin\theta/\lambda$ region.

The symmetry in a Patterson map is related to the symmetry in the electron-density map, but it is not necessarily the same. For instance, screw axes in the real cell become non-screw axes in the Patterson cell, because all interatomic vectors start at the origin. It is possible, however, to distinguish between screw axes and non-screw axes by the concentration of peaks in the Patterson

map. For instance, the consequence of a twofold symmetry axis along **b** is the presence of a large number of peaks in the $(u0w)$ plane of the Patterson map. For a screw axis with translation $\frac{1}{2}$ along **b**, the peaks lie in the $(u\frac{1}{2}w)$ plane. Such planes are called Harker planes (Harker, 1936). Peaks in Harker planes usually form the start of the interpretation of a Patterson map. Harker lines result from mirror planes, which do not occur in macromolecular crystal structures of biological origin.

Despite the improvements that can be made to the Patterson function, for structures containing atoms of nearly equal weight its complete interpretation can only be achieved for a restricted number of atoms per cell unless some extra information is available. Nowadays, most structure determinations of small compounds are based on direct methods for phase determination. However, these may fail for structures showing strong regularity. In these cases, Patterson interpretation is used as an alternative tool, sometimes in combination with direct methods. It is interesting to see that the value of the Patterson function has shifted from the small-compound field to macromolecular crystallography, where it plays an extremely useful role:

(1) in the isomorphous replacement method, the positions of the very limited number of heavy atoms attached to the macromolecule can be derived from a difference Patterson map, as mentioned earlier in this section;
(2) anomalous scatterers can be located by calculating a Patterson map with coefficients $[|F_{PH}(\mathbf{h})| - |F_{PH}(-\mathbf{h})|]^2$, in which $|F_{PH}(\mathbf{h})|$ is the structure-factor amplitude of the protein containing the anomalous scatterer;
(3) molecular replacement is based on the property that the Patterson map is a map of vectors between atoms in the real structure, combined with the fact that such a vector map is (apart from a rotation) similar for two homologous structures: the unknown and a known model structure.

I am greatly indebted to Aafje Looyenga-Vos for critically reading the manuscript and for many useful suggestions.

References

Burzlaff, H. & Zimmermann, H. (2005). *Bases, lattices, Bravais lattices and other classifications*. In *International Tables for Crystallography*, Vol. A. *Space-Group Symmetry*, edited by Th. Hahn, ch. 9.1. Heidelberg: Springer.

Drenth, J. (1999). *Principles of Protein X-ray Crystallography*. New York: Springer-Verlag.

Haas, C. & Drenth, J. (1995). *The interaction energy between two protein molecules related to physical properties of their solution and their crystals and implications for crystal growth*. *J. Cryst. Growth*, **154**, 126–135.

Harker, D. (1936). *The application of the three-dimensional Patterson method and the crystal structures of proustite, Ag_3AsS_3, and pyrargyrite, Ag_3SbS_3*. *J. Chem. Phys*. **4**, 381–390.

Heitler, W. G. (1966). *The Quantum Theory of Radiation*, 3rd ed. Oxford University Press.

Hönl, H. (1933). *Atomfaktor für Röntgenstrahlen als Problem der Dispersionstheorie (K-Schale)*. *Ann. Phys*. **18**, 625–655.

International Tables for Crystallography (2008). Vol. B. *Reciprocal Space*, edited by U. Shmueli, 3rd ed. Heidelberg: Springer.

International Tables for Crystallography (2004). Vol. C. *Mathematical, Physical and Chemical Tables*, edited by E. Prince. Dordrecht: Kluwer Academic Publishers.

International Tables for Crystallography (2005). Vol. A. *Space-Group Symmetry*, edited by Th. Hahn. Heidelberg: Springer.

James, R. W. (1965). *The Optical Principles of the Diffraction of X-rays*, p. 135. London: G. Bell and Sons Ltd.

Kauzmann, W. (1957). *Quantum Chemistry*. New York: Academic Press.

Klein, O. & Nishina, Y. (1929). *Über die Streuung von Strahlung durch freie Elektronen nach der neuen relativistischen Quantendynamik von Dirac*. *Z. Phys*. **52**, 853–868.

Patterson, A. L. (1934). *A Fourier series method for the determination of the components of interatomic distances in crystals*. *Phys. Rev*. **46**, 372–376.

Waser, J. (1955). *Symmetry relations between structure factors*. *Acta Cryst*. **8**, 595.

Wilson, A. J. C. (1942). *Determination of absolute from relative X-ray intensity data*. *Nature (London)*, **150**, 151–152.